AD NUMBER

AD911292

NEW LIMITATION CHANGE

TO

Approved for public release, distribution unlimited

FROM

Distribution authorized to U.S. Gov't. agencies only; Test and Evaluation; MAY 1973. Other requests shall be referred to Air Force Armament Lab., Eglin AFB, FL 32542.

AUTHORITY

AFAL ltr, 11 Mar 1974

TECHNICAL REPORT AFATL-TR-73-110

MK82 BALLUTE RETARDER SYSTEM STRUCTURAL QUALIFICATIONS

Wiley J. Robinson
AIRCRAFT COMPATIBILITY AND WEAPONS FLIGHT DYNAMICS BRANCH
PRODUCT ASSURANCE DIVISION

MAY 1973

FINAL REPORT: June to August 1972

AIR FORCE ARMAMENT LABORATORY
AIR FORCE SYSTEMS COMMAND • UNITED STATES AIR FORCE
EGLIN AIR FORCE BASE, FLORIDA

UNCLASSIFIED
Security Classification

DOCUMENT CONTROL DATA - R & D

(Security classification of title, body of abstract and indexing annotation must be entered when the overall report is classified)

1. ORIGINATING ACTIVITY (Corporate author)	2a. REPORT SECURITY CLASSIFICATION
Product Assurance Division Air Force Armament Laboratory Eglin Air Force Base, Florida 32542	Unclassified
	2b. GROUP

3. REPORT TITLE

MK82 BALLUTE RETARDER SYSTEM STRUCTURAL QUALIFICATIONS

4. DESCRIPTIVE NOTES (Type of report and inclusive dates)

Final Report (June - August 1972)

5. AUTHOR(S) (First name, middle initial, last name)

Wiley J. Robinson

6. REPORT DATE	7a. TOTAL NO. OF PAGES	7b. NO. OF REFS
M / 1973	55	

8a. CONTRACT OR GRANT NO.	9a. ORIGINATOR'S REPORT NUMBER(S)
b. PROJECT NO. 15591301	AFATL-TR-73-110
c.	9b. OTHER REPORT NO(S) (Any other numbers that may be assigned this report)
d.	

10. DISTRIBUTION STATEMENT

Distribution limited to U. S. Government agencies only; this report documents test and evaluation; distribution limitation applied May 1973. Other requests for this document must be referred to the Air Force Armament Laboratory (DLGC), Eglin Air Force Base, Florida 32542.

11. SUPPLEMENTARY NOTES	12. SPONSORING MILITARY ACTIVITY
Available in DDC	Air Force Armament Laboratory Air Force Systems Command Eglin Air Force Base, Florida 32542

13. ABSTRACT

When the MK82 ballute retarder system was received from the contractor to be qualified for flight testing, certain areas of analyses usually required had been omitted from the data package. This report details the completed in-house design work and the ground testing necessary to verify the analyses and to qualify the retarder system.

DD FORM 1 NOV 68 1473

UNCLASSIFIED
Security Classification

14. KEY WORDS	LINK A		LINK B		LINK C	
	ROLE	WT	ROLE	WT	ROLE	WT
Baliute						
Retarder System						
MK82 Bomb						
Structural Analysis						
Vibration Testing						

PREFACE

This technical report covers work performed in support of Project 15591301 during the period 16 June through 31 August 1972 by the Structural Dynamics Team at the Air Force Armament Laboratory.

Portions of this report are based on information obtained from the following books:

David J. Perry: Aircraft Structures, McGraw-Hill, Copyright 1950.

Ramond J. Roark: Formulas for Stress and Strain, Fourth Edition. McGraw-Hill, 1965.

S. Timoshinko: Strength of Materials. "Part 1, Elementary Theory and Problems." Third Edition, D. Van Nostrand Co., Inc., 1958.

This technical report has been reviewed and is approved.

R. L. FETTY, Colonel, USAF
Chief, Product Assurance Division

(The reverse of this page is blank)

TABLE OF CONTENTS

(The reverse of this page is blank)

SECTION I

INTRODUCTION

When the data package for the MK82 ballute (BALLoon-parachUTE) retarder system was received from the contractor by the Air Force Armament Laboratory (AFATL) for evaluation, the captive flight loads data and the procedures used during vibration testing were not complete. Consequently, an in-house program was initiated to qualify the MK82 ballute retarder system.

The specific area to be investigated was the main attachment joint between the tail fin and the basic bomb body. The data package did not include the acceleration load factors encountered during captive flight maneuvers, and also, a material having brittle properties had been used for the joint fitting.

SECTION II

DESCRIPTION AND MASS PROPERTIES

The purpose of the MK82 ballute retarder system is to reduce the descent rate of the MK82 500-pound general purpose bomb. Two sizes of ballutes are considered for this objective. One ballute, approximately 29 inches in diameter, is designed to provide a 400 ft/sec terminal velocity for the MK82 bomb, which is intended for mining applications. The second ballute, approximately 41 inches in diameter, is designed to provide a terminal velocity of 238 ft/sec for the bomb and is intended to replace the MK15 high drag fin. Both ballute retarder systems are composed of a finned cylindrical canister containing the stowed ballute, the actuating mechanism, and the fittings for attachment to the bomb (Figures 1 to 3). After the bomb separates from the parent aircraft, the aft closure disk is released and is pulled backwards by aerodynamic forces. Thus the ballute, which is attached to the disk, is extracted from the canister and then inflated by ram air. The physical property data for the MK82 ballute retarder system used in these flight tests are provided in Table 1.

TABLE 1. PHYSICAL PROPERTIES FOR THE MK82 BALLUTE RETARDER SYSTEM

COMPONENT	WEIGHT (Pounds)	CENTER OF GRAVITY (Inches Aft of Sta. 0.0)	PITCH AND YAW MOMENTS OF INERTIA (Slug-Ft^2)	ROLL MOMENT OF INERTIA (Slug-Ft^2)
Body	301.0	35.86	22.797	1.789
Explosive	192.0	40.18	9.840	0.518
Fuse (Forward)	5.0	6.00	1.360	0.003
Fuse (Aft)	5.0	62.65	0.577	0.003
Canister	33.9	79.88	11.240	0.135
Ballute				
29-inch	6.0	82.50	2.190	0.010
41-inch	13.0	83.5	2.190	0.010
Latch	3.2	91.40	1.720	0.011
Clamp	12.5	66.15	1.660	0.043
Total				
29-inch Ballute	558.6	41.486	51.38	2.51
41-inch Ballute	565.6	41.993	53.94	2.53

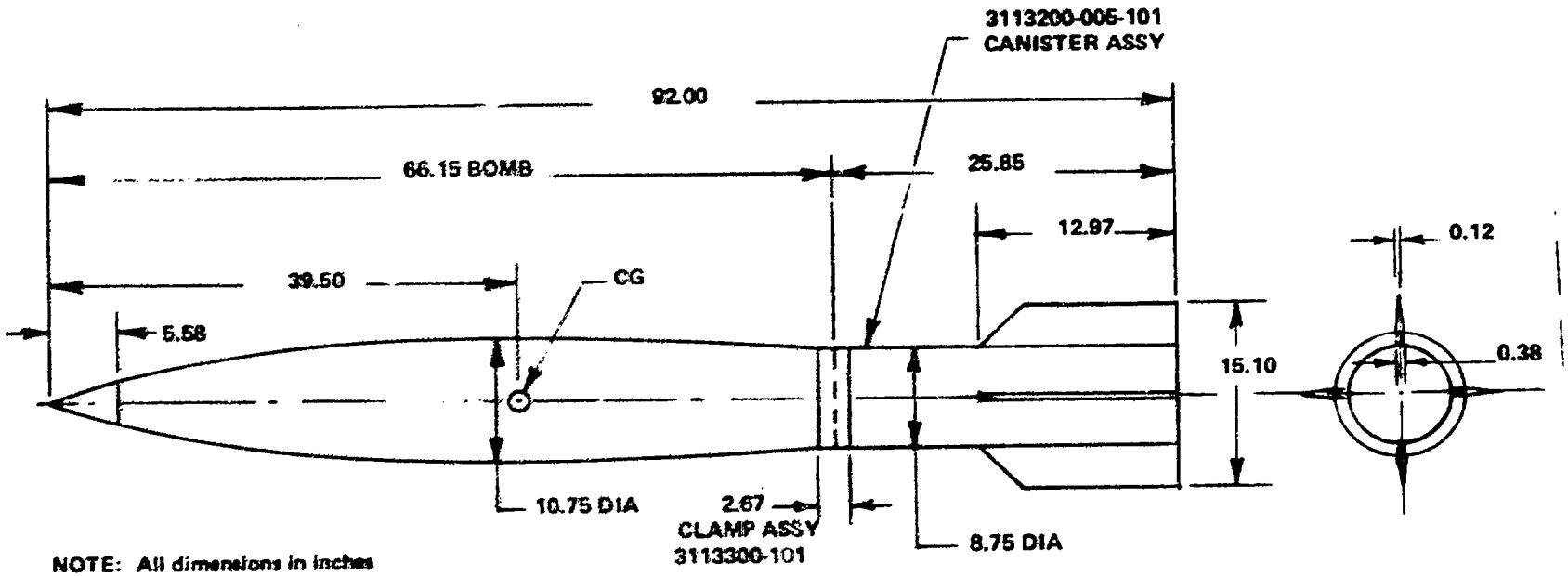

Figure 1. Dimensions of MK82 Bomb with Ballute Stowed

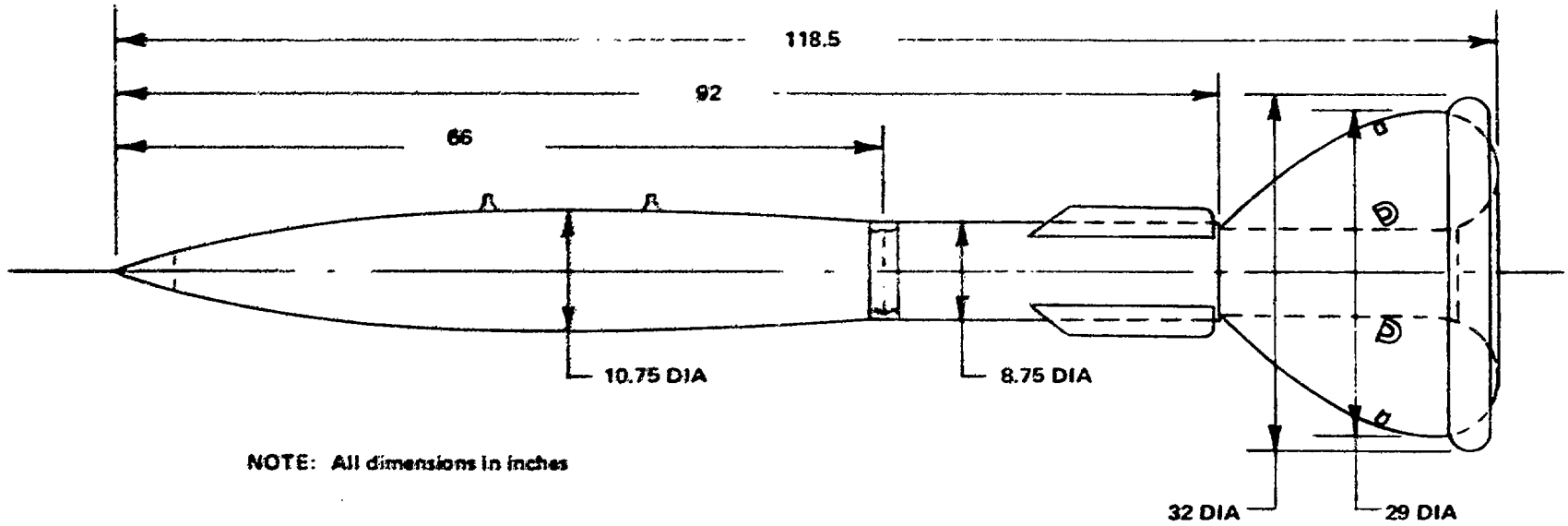

Figure 2. Dimensions of MK82 with Ballute Deployed (29 inches diameter)

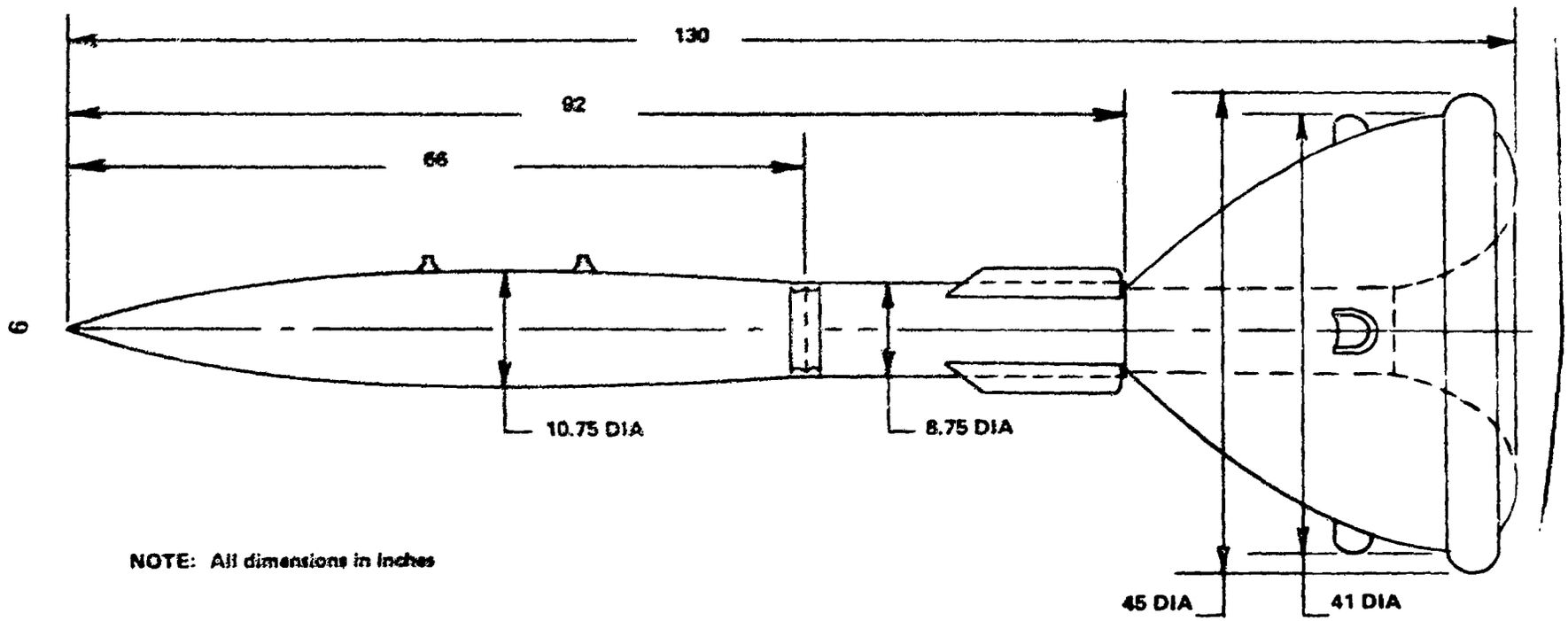

Figure 3. Dimensions of MK82 with Ballute Deployed (41 inch diameter)

SECTION III

LOADS ANALYSIS SECTION

This section details the design loads for the critical conditions of free flight and captive carriage; including captive maneuver, catapult launch, and arrested landing.

1. AERODYNAMIC DATA

The normal force coefficient (C_n), the center of pressure (inches aft of the MK82 base plate, or tail fin intersection (X_{cp})), and the pitching moment coefficient (C_{mcg}), were calculated for several angles of attack (α). The angle of attack is measured between the weapon longitudinal axis and the relative wind vector.

These aerodynamic coefficients (C_n, C_{mcg}, and X_{cp}) were used in determining aerodynamic loads provided in Tables 2 to 4. All of the coefficients are based upon the maximum body diameter and consider the influence of fin-to-body effects and body-to-fin effects. The methodologies employed to obtain the aerodynamic coefficients were extracted from Reference 1.

2. CAPTIVE LOADS

Three basic conditions must be considered in defining the most critical loads for the MK82 ballute munition when attached to the carrier aircraft: (a) maneuvering flight loads, (b) catapult launch, and (c) arrested landing. The computer program AIRSAR (Reference 2) was used to evaluate the many thousands of load permutations that could be developed by the three conditions.

The AIRSAR program uses the design criteria outlined in Reference 3. Over 26,000 possible loading combinations resulted from use of the different angles of attack, angles of sideslip, pitching accelerations, yawing accelerations, vertical load factor, longitudinal load factor, lateral load factor, and varying dynamic pressures. The combinations include flight, arrested landing, and catapulting conditions for externally carried weapons on wings and fuselage (Tables 5 and 6).

The inputs to AIRSAR are aerodynamic data, maximum dynamic pressure, mass property data, and geometry of the suspension system. The outputs are loads at the lug and swaybrace interface points, plus the net loads acting at the weapon center of gravity.

Lug and sway brace geometry and sign convention used in this program are depicted in Figures 4 and 5, respectively.

Appendix A details the theoretical methods of solving the interface loads. A synopsis of the maximum interface loads conditions are provided in Table 7.

References:
1. Dr. S. S. Chin: Missile Configuration Design. McGraw-Hill, 1961.
2. W. W. Dyess: A User's Manual for AIRSAR (Airborne Stores and Racks). Air Force Armament Laboratory, ATII-TN-70-1, May 1970.
3. General Design Criteria for Airborne Stores and Associated Suspension Equipment, Military Specification MIL-A-8591D, 2 January 1968.

The following symbols are used in the tables and figures in this subsection.

SYMBOL	DEFINITION
W (lb)	Weight of store
I ($lb\text{-}in^2$)	Mass moment of inertia of store
q	Varying dynamic pressure
n_z	Vertical load factor
n_x	Longitudinal load factor
n_y	Lateral load factor
α (degrees)	Angle of attack
β (degrees)	Angle of sideslip
$\ddot{\theta}$ (rad/sec)	Pitching acceleration
$\ddot{\psi}$ (rad/sec)	Yawing acceleration
P_z (lb)	Total vertical load at store cg
P_x (lb)	Total longitudinal load at store cg
P_y (lb)	Total lateral load at store cg
M_y (in-lb)	Total pitching moment about store cg
M_z (in-lb)	Total yawing moment about store cg
ℓ (inch)	Total length of store
ℓ_a (inch)	Distance from aft lug to store cg
ℓ_f (inch)	Distance from forward lug to store cg
$\bar{\ell}_a$ (inch)	Distance from aft sway-brace to store cg
$\bar{\ell}_f$ (inch)	Distance from forward sway-brace to store cg
r (inch)	radius of store
c (inch)	Vertical distance between upper surface of store and a line on the cross bar of the lug where fore and aft loads are reacted.
h (inch)	Vertical distance between the upper surface of the store and the point on the lug where a side load reaction may be provided.
e (inch)	Vertical distance between the store cg and the intersection of the lines of action of the sway-braces.

SYMBOL	DEFINITION
B_a (radians)	Angle between the vertical plane and the line-of-action of the aft sway-braces in a fore-and-aft view
B_f (radians)	Angle between the vertical plane and the line-of-action of the forward sway-braces in a fore-and-aft view.
R_z^f (lb)	Reaction in Z-direction at forward lug.
R_z^a (lb)	Reaction in Z-direction at aft lug
R_x^a (lb)	Reaction in X-direction at aft lug
R_y^f (lb)	Reaction in Y-direction at forward lug
R_y^a (lb)	Reaction in Y-direction at aft lug.
C_n	Normal force coefficient
C_m	Pitching moment coefficient
R_{SB}^a	Maximum loads on aft sway brace
R_{SB}^f	Maximum loads on forward sway brace

TABLE 2. AERODYNAMIC COEFFICIENTS FOR THE CANISTER SECTION AT MACH 0.9

α (degrees)	C_n	C_{mcg}	X_{cp}
0	0	0	
5	0.27	- 1.03	3.40
10	0.67	- 2.53	3.38
15	1.17	- 4.43	3.39
20	1.75	- 6.62	3.38
30	3.01	-11.33	3.37
40	4.18	-15.74	3.37
50	5.13	-19.17	3.35
60	5.75	-21.43	3.34
70	6.11	-22.63	3.32
80	6.18	-22.89	3.32
90	6.16	-22.75	3.31

TABLE 3. AERODYNAMIC COEFFICIENTS FOR THE CANISTER SECTION AT MACH 1.2			
α (degrees)	C_n	C_{mcg}	X_{cp}
0	0	0	
5	0.29	- 1.17	3.61
10	0.70	- 2.83	3.63
15	1.22	- 4.89	3.59
20	1.82	- 7.25	3.57
30	3.15	-12.43	3.53
40	3.51	-17.61	3.50
50	5.62	-21.78	3.47
60	6.13	-23.59	3.45
70	6.15	-23.50	3.42
80	5.98	-22.76	3.41
90	5.92	-22.49	3.42

TABLE 4. AERODYNAMIC COEFFICIENTS FOR THE COMPLETE MK82 WITH STOWED BALLUTE RETARDER SYSTEM				
α (degrees)	Mach 0.9		Mach 1.2	
	C_n	C_m	C_n	C_m
5	0.42	- 0.61	0.45	- 0.75
10	1.06	- 1.66	1.12	- 1.94
15	1.89	- 3.07	2.01	- 3.49
20	2.88	- 4.76	3.09	- 5.31
30	5.20	- 8.45	5.74	- 9.30
40	7.73	-11.87	9.01	-13.17
50	10.25	-14.41	12.31	-16.08
60	12.53	-15.94	14.43	-17.19
70	14.35	-16.68	15.34	-16.97
80	15.18	-16.87	15.56	-16.49
90	15.32	-17.23	15.56	-16.67

TABLE 5. DESIGN LOAD CONDITIONS - WING MOUNTED WEAPON

LOAD FACTOR ENVELOPE POINT (Reference 2)	n_z	n_y	n_x	$\ddot{\theta}$	$\ddot{\psi}$	β_s	α_s
FLIGHT CONDITIONS							
1, 2	-11.5	±1.5	±1.5	±4	±2	$\pm\frac{3000}{q}$	$-3, 0, \frac{38000}{q}-3, -\frac{38000}{q}$
3, 4	+6.0	±1.5	±1.5	±4	±2	$\pm\frac{3000}{q}$	$-3, 0, \frac{22800}{q}, -\frac{22800}{q}-3$
5	+1.0	-7.5	±1.5	±4	±2	$\pm\frac{13000}{q}$	$\frac{100}{\sqrt{q}}, \frac{100}{\sqrt{q}}-3, -\frac{(15200+100\ q)}{q}-3, -\frac{(15200+100\ q}{q}$
6	-6.0	-7.5	±1.5	±4	±2	$\pm\frac{13000}{q}$	$0, -3, \frac{30400+100\sqrt{q}}{q}, \frac{30400+100\sqrt{q}}{q}-3$
ARRESTED LANDING CONDITIONS							
1	-12.0	±5.0	±2.0	±25	±6		
2	-12.0	±5.0	-2.5	±25	±6		
3	+4.0	±5.0	+2.0	±25	±6		
4	+4.0	±5.0	-3.0	±25	±6		
5	+2.0	±5.0	-9.0	±25	±6		
6	-6.0	±5.0	-9.0	±25	±6		
CATAPULTING CONDITIONS							
1	-5.0	±2.5	+9.0	±15	±4		
2	-5.0	±2.5	-2.0	±15	±4		
3	+1.5	±2.5	+8.0	±15	±4		
4	+1.5	±2.5	-2.0	±15	±4		

NOTE: β_s and α_s are not considered for arrested landing and catapulting conditions.

TABLE 6. DESIGN LOAD CONDITIONS - FUSELAGE MOUNTED WEAPON

LOAD FACTOR ENVELOPE POINT (Reference 2)	n_z	n_y	n_x	$\ddot{\theta}$	$\ddot{\psi}$	β_s	α_s
FLIGHT CONDITIONS							
1, 3	-3.67	±1.5	±1.5	±4	±2	$\pm\frac{13000}{q}$	$0, -3, \frac{38000}{q}, \frac{38000}{q} - 3$
2, 4	+4.0	±1.5	±1.5	±4	±2	$\pm\frac{13000}{q}$	$0, -3, \frac{30400}{q}, \frac{30400}{q} - 3$
ARRESTED LANDING CONDITIONS							
1, 2	-3.0	±1.5	±2.0	±12	±6		
3, 4	+3.5	±1.5	±2.0	±12	±6		
5	+1.5	±1.5	-8.0	±12	±6		
6	-3.0	±1.5	-8.0	±12	±6		
CATAPULTING CONDITIONS							
1	-5.0	±1.0	+7.0	±12	±6		
2	-5.0	±1.0	-2.0	±12	±6		
3	-1.0	±1.0	+7.0	±12	±6		
4	+1.0	±1.0	-2.0	±12	±6		

NOTE: β_s and α_s are not considered for arrested landing and catapulting conditions.

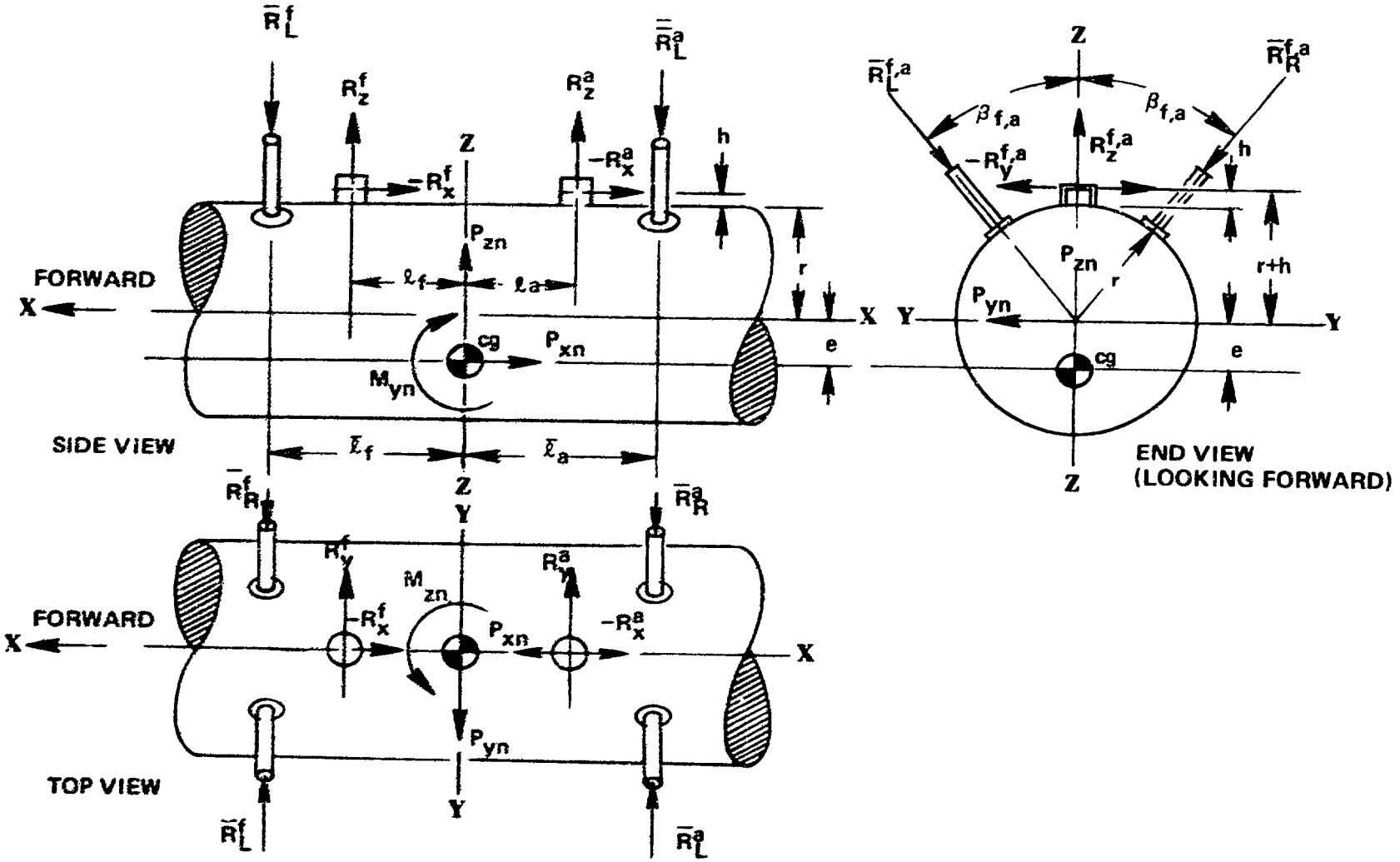

Figure 4. Lug and Sway Brace Geometry

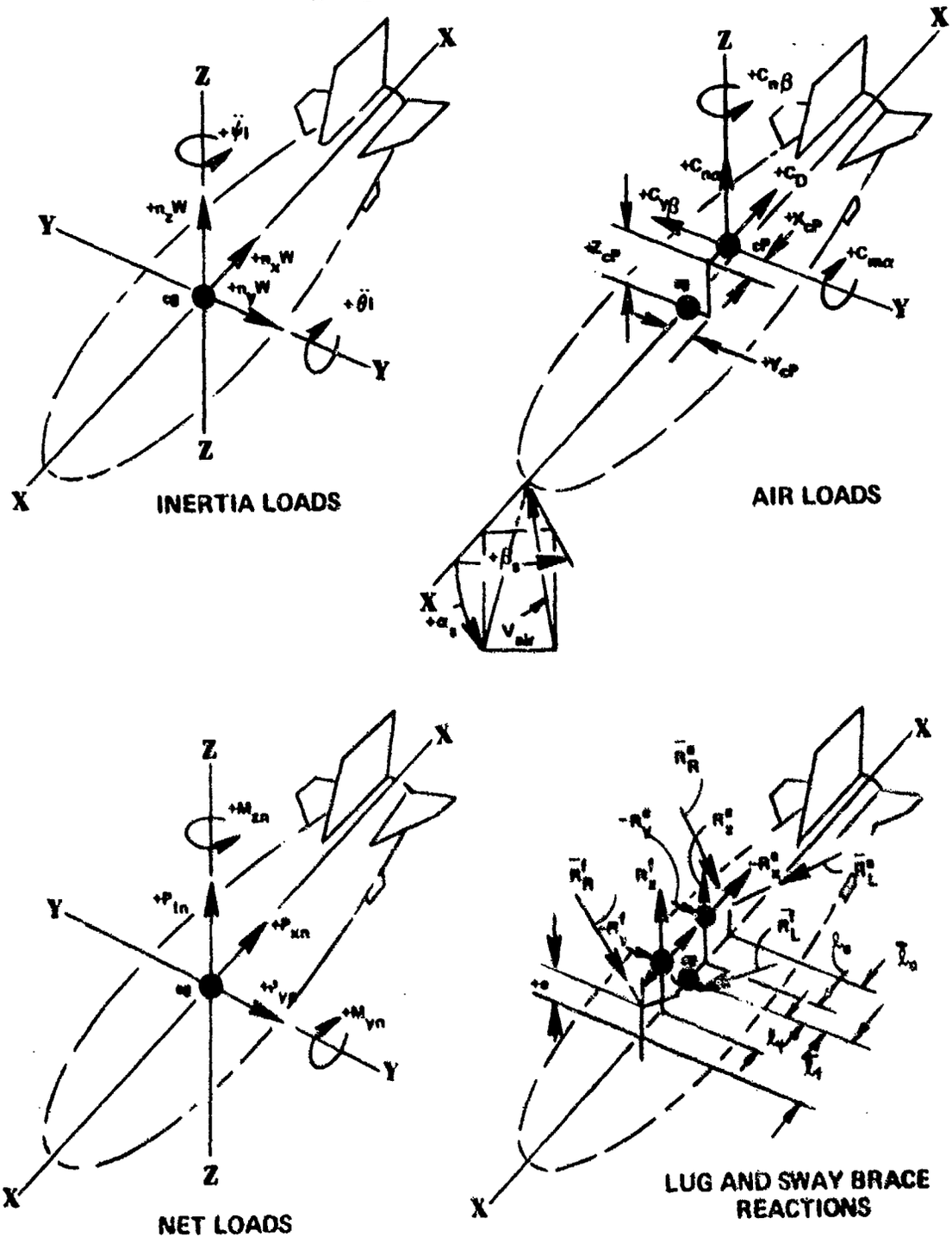

Figure 5. Sign Conventions

TABLE 7. CRITICAL CAPTIVE LOADS SUMMARY						
LOAD CONDITION	49	50	59	72	2233	2425
MACH NO.	1.2	1.2	1.2	1.2	N/A	N/A
q	2000	2000	2000	2000	N/A	N/A
α	2.24	2.24	- 12.84	17.43	N/A	N/A
β	6.5	-6.5	6.5	-6.5	N/A	N/A
C_n	0.179	0.179	-1.03	1.39	N/A	N/A
C_Y	0.520	0.520	0.520	-0.52	N/A	N/A
C_a	0.100	0.100	0.100	0.100	N/A	N/A
C_m	-0.335	-0.335	1.93	-2.62	N/A	N/A
C_{nn}	-0.975	-0.975	-0.975	0.975	N/A	N/A
n_y	7.5	7.5	7.5	7.5	2.5	-5.0
n_z	1.00	1.00	1.00	-6.0	-5.0	-12.0
n_x	1.5	1.5	-1.5	1.5	9.0	2.0
$\ddot{\theta}$	4	4	4	4	15	25
$\ddot{\psi}$	2	2	-2	2	4	6
R_x^f	0	883	0	883	4545	0
R_x^a	883	0	-631	0	0	1010
R_y^f	0	0	0	0	0	0
R_y^a	0	0	0	0	0	0
R_z^f	3425	5967	1086	9024	4666	5390
R_z^a	6338	19.14	9232	0	566	6085
$*R_{SB}^f$	4063	5560	3850	5560	1781	2817
$*R_{SB}^a$	6663	1851	6663	2422	1206	3147

*Only the maximum values are presented.

3. FREE FLIGHT LOADS

Immediately after release of the munition, large angular excursions of the weapon may be encountered. This section details the fin loadings during these pertubations. The MK82 basic bomb body is considered structurally adequate, based on previous analysis and extended flight testing; therefore, the distributed body loads are not evaluated. Figure 6 illustrates the loads imposed on the body, resulting from aerodynamic and dynamic reaction loads.

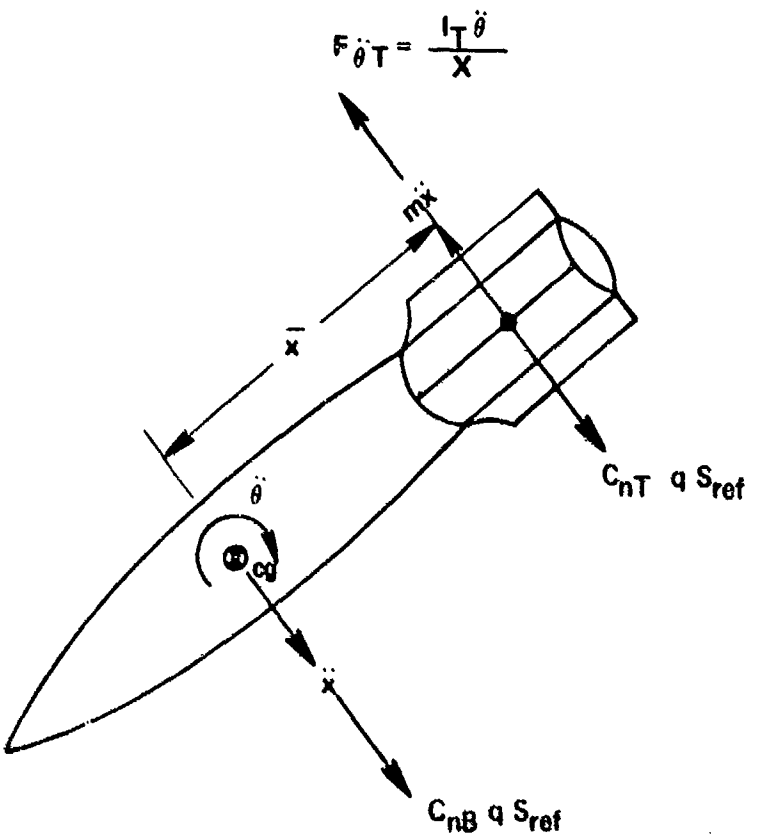

Figure 6. Aerodynamic and Inertial Loading Diagram

The following symbols are used in this section to discuss free flight loads.

SYMBOL	DEFINITION
I_T	Total inertia of the tail section
I_o	Segment inertias about the mass centroids
I_B	Inertia of the entire body (bomb + tail)

SYMBOL	DEFINITION
$M_{\ddot{\theta}}$	Dynamic moment for the entire body about the cg
$\ddot{\theta}$	Angular acceleration rate
C_{mcg}	Pitching moment coefficient about cg
q	dynamic pressure
S_{ref}	Reference area
$\bar{c}$	Reference length
$F_{\ddot{\theta}T}$	Forces of the tail due to angular acceleration
M_T	Mass of the tail section
$\bar{X}$	Mass of the tail section
$F_{\ddot{X}B}$	Translational force at the body cg
M_B	Mass of the body
C_{nB}	Normal force coefficient of the body
$F_{\ddot{X}T}$	Translational force of the tail
F_T	Total force on the tail

The mass moment of inertia (pitch = yaw) for the tail section can be defined as follows:

$$I_T = M_T \bar{X}^2 + I_o$$

$$I_o = I(\text{clamp}) + I(\text{ballute}) + I(\text{latch}) + I(\text{can}) = 3468.8 \text{ lb-in}^2$$

or

$$I_o = 0.748 \text{ slug-ft}^2$$

$$M_{\ddot{\theta}} = I_B \ddot{\theta}$$

$$M_{\ddot{\theta}} = (C_{mcg})\ q\ (S_{ref})\ \bar{c}$$

$$\ddot{\theta} = \frac{(C_{mcg})\, q\, (S_{ref})\, \bar{c}}{I_B}$$

$$F_{\ddot{\theta}T} = \frac{\ddot{\theta} I_T}{\bar{X}} = \ddot{\theta}\left(\frac{M_T \bar{X}^2}{\bar{X}}\right) + \ddot{\theta}\left(\frac{I_o}{\bar{X}}\right) = \ddot{\theta}\left(M_T \bar{X} + \frac{I_o}{\bar{X}}\right)$$

$$F_{\ddot{\theta}T} = \frac{(C_{mcg})\, q\, (S_{ref})\ \bar{c}}{I_B}\left(M_T\ \bar{X} + \frac{I_o}{\bar{X}}\right)$$

$$F_{\ddot{X}B} = M_B \ddot{X}$$

$$F_{\ddot{X}B} = (C_{nB})\, q\, (S_{ref}) = M_B \ddot{X}$$

$$\ddot{X}_B = \frac{(C_{nB})\ q\ (S_{ref})}{M_B}$$

$$F_{\ddot{X}T} = M_T \left[\frac{(C_{nB})\, q\, (S_{ref})}{M_B}\right]$$

$$F_{(tail)} = F_{\ddot{\theta}T} = F_{\ddot{X}T}$$

$$= \frac{(C_{mcg})\, q\, (S_{ref})\ \bar{c}}{I_B}\left(M_T \bar{X} + \frac{I_o}{\bar{X}}\right) + M_T \left[\frac{(C_{nB})\, q\, (S_{ref})}{M_B}\right]$$

$$F_{(aero)} = (C_{nT})\, q\, (S_{ref})$$

$$F_T = F_{(aero)} \cdot F_{(tail)}$$

$$F_T = (C_{nT})\, q\, (S_{ref}) \cdot \frac{(C_{mcg})\, q\, (S_{ref})\ \bar{c}}{I_B}\left(M_T \bar{X} + \frac{I_o}{\bar{X}}\right) + M_T \left[\frac{C_{nB})\, q\, (S_{ref})}{M_B}\right]$$

Two specific conditions were evaluated: Mach 1.2 and Mach 0.9. The data used in the calculations are provided in Table 8.

TABLE 8. FLIGHT CONDITION DATA

Mach	0.9	1.2
q	1200 lb/ft^2	2000 lb/ft^2
S_{ref}	0.63 ft^2	0.63 ft^2
$\bar{c}$	0.896 ft	0.896 ft
I_B	57.4 slug-ft^2	57.4 slug-ft^2
M_T	2.08 slug	2.08 slug
$\bar{X}$	3.329 ft	3.429 ft
I_o	0.748 slug-ft^2	0.748 slug-ft^2
C_{nB}	14.35	15.34
M_B	16.77 slug	16.77 slug
C_{nT}	6.11	6.15

F_T = 1864 pound limit @ Mach = 0.9

F_T = 2899 pound limit @ Mach 1.2

SECTION IV

STRESS ANALYSIS

The major concern of the effort discussed in this report was the band clamp assembly that retains the entire fin and ballute assembly. All other portions of the structure have adequate strength capabilities even at the increased loads used in the analyses.

The following symbols are used in this section to discuss the stress analysis.

SYMBOL	DEFINITION
σ_b	Bending stress lb/in^2
σ_s	Shearing stress lb/in^2
F_{tu}	Allowable tensile ultimate strength lb/in^2
F_{ty}	Allowable tensile yield strength lb/in^2
F_{su}	Allowable shear ultimate strength lb/in^2
F_{sy}	Allowable shear yield strength lb/in^2
R_{bu}	Bending index factor, ultimate
R_{by}	Bending index factor, yield
R_{su}	Shear index factor, ultimate
R_s	Shear index factor, yield
MS	Margin of safety
T	Thickness of material

The band clamp consists of two inner U-shaped jaws with an external strap (Figure 7). The jaws are designed to be the primary load carrying members while the strap is designed to secure the jaws and will react only to tension loads. The strap was preloaded by torquing the two trunion bolts and it was assumed that until this preload was exceeded, there would be no increase in the load on the external strap. This assumption was verified by the static loads test discussed in Section V.

1. SHELL

The maximum side load that can be experienced, as derived in Section III, is

$$N_s = 2899 \text{ lb.}$$

The maximum bending moment will be

$$M_s = N_s (X_{cp} - X_s) = 2899 (14.39 - 3.40) = 31,860 \text{ in-lb}$$

For conservatism, the maximum stress in the shell is assumed to occur at the access holes.

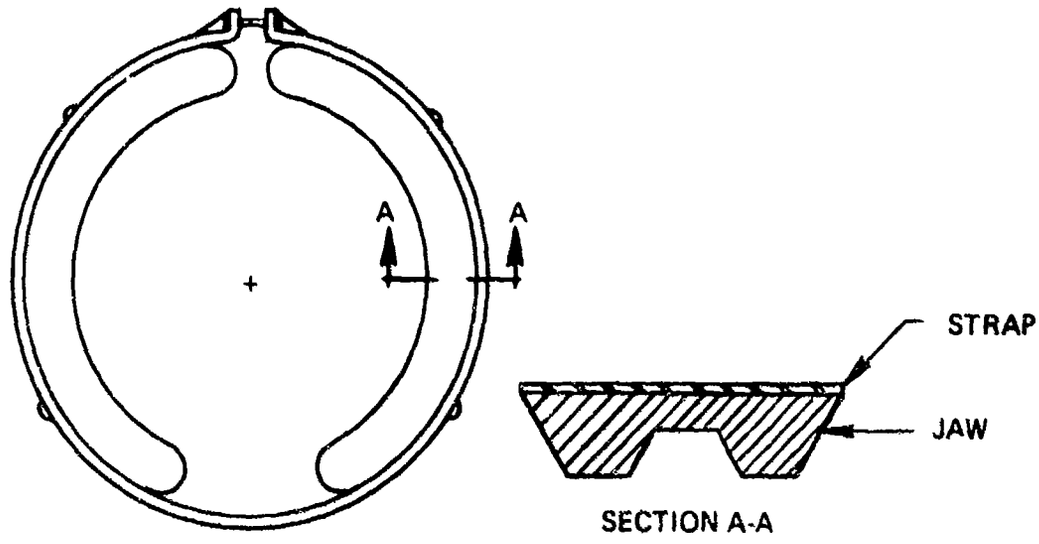

Figure 7. Band Clamp Assembly

Therefore,

$$\sigma_b = \frac{M_s z}{I}$$

Where

$I = 54.77\ in^4$

$z = 4.375\ in^3$

and

$\sigma_b = 2544.7\ lb/in^2$

$$\sigma_s = \frac{2899}{\pi (4.375)\ (2)\ (0.375)\ (0.3)} = 938\ lb/in^2$$

A minimum of 33 percent of the strength must remain for aluminum castings. The following requirements apply to the shell:

Material = Aluminum casting

$F_{tu} = 30{,}000\ lb/in^2$

$F_{ty} = 20{,}000\ lb/in^2$

$F_{su} = 25{,}000\ lb/in^2$

$F_{sy} = 16{,}700\ lb/in^2$

$$R_{bu} = \frac{\sigma_{bu}}{F_{tu}} \qquad R_{su} = \frac{\sigma_{su}}{F_{su}}$$

$$R_{by} = \frac{\sigma_b}{F_{ty}} \qquad R_s = \frac{\sigma_s}{F_s}$$

$$R_{bu} = \frac{2544.7\ (1.5)}{30000} = 0.127$$

$$R_{su} = \frac{938\ (1.5)}{25000} = 0.056$$

$$MS_u = \frac{1}{R_{bu} + R_{su}} \cdot 1 = 4.46 \quad \text{High}$$

$$R_{by} = \frac{2544.7\ (1.15)}{20000} = 0.146$$

$$R_{sy} = \frac{938\ (1.15)}{16700} = 0.065$$

$$MS_y = 3.74 \quad \text{High}$$

2. CLAMP ASSEMBLY (Drawing 311300-001)

The assumption was made that the strap would be reacting only to the tension loads needed for securring the jaws. However, it was known that there would be some degree of transfer of loads from the jaws to the strap. This degree of transfer would depend on machine tolerances of the clamp jaws and bomb attachment grooves, flexures of the jaws, preloading of the strap, dynamics, etc. The analysis of these variables is too difficult to obtain any meaningful load distribution predictions, and for this reason, the static loads test presented in Section V was deemed necessary. For analysis of the clamp, all joint loads are assumed to be in the jaws of the clamp. This method of approach is conservative for the jaws design.

A cross section of the clamp jaws where the critical loads will occur is depicted in Figure 8. In evaluating this cross section at the elastic axis A-A, the applied moment is

$$M = 0.38\ P_s + 0.62\ P_v$$

Where P_s and P_v are applied loads, and $P_s = P_v$,

$$P_s = 2899 \text{ lb/in}$$

and

$$M = 0.38\ (P_s) + 0.62\ (P_v)$$

$$M = 2899 \text{ in lb/in}$$

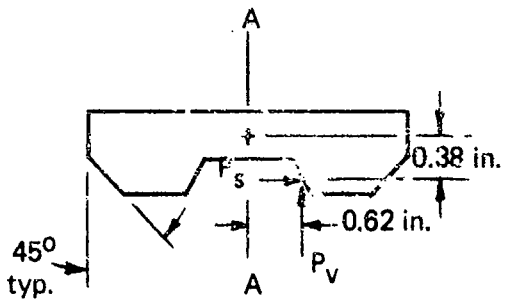

Figure 8. Jaw Critical Cross Section

$$P_s = 2899 \text{ lb/in}$$

$$\sigma_b = \frac{6M}{t^2} = \frac{6\,(2899)}{(0.469)^2} = 79078 \text{ lb/in}^2$$

$$\sigma_s = \frac{P_s}{t} = \frac{2899}{0.469} = 6181 \text{ lb/in}^2$$

Material: 4142 H Alloy

$$F_{tu} = 140000 \text{ lb/in}^2$$

$$F_{su} = 70000 \text{ lb/in}^2$$

$$R_{bu} = \frac{\sigma_{bu}}{F_{tu}}$$

$$R_{su} = \frac{\sigma_{su}}{F_{su}}$$

$$\sigma_{bu} = 118617 \text{ lb/in}^2$$

$$\sigma_{su} = 9272 \text{ lb/in}^2$$

$$R_{bu} = 0.847$$

$$R_{su} = 0.132$$

$$MS = \frac{1}{R_{bu} + R_{su}} - 1 = 1.02 - 1 = 0.02$$

SECTION V

STATIC LOADS TEST

As stated in Section IV, a static loads test was required to verify the ability of the band retaining clamp to withstand the applied loads, In addition, the margins of safety as calculated were low and needed verification by a static loads tests.

The test was completed in two phases. The first phase was to apply the loads that would be experienced at Mach 0.9, and the second phase was to be at Mach 1.2. This approach was used so that, if the item passed at Mach 0.9 but failed at Mach 1.2, flight testing could be completed, based on the results of the testing at Mach 0.9.

All testing was performed at an atmospheric pressure of 29.0 ($\pm$2) inches of mercury absolute, a temperature of 88 ($\pm$ 10^{o}) F, and a relative humidity not exceeding 90 percent.

All test equipment was calibrated and controlled, and all reference standards used for calibration are supported by certificates, reports, or data sheets attesting to the date, accuracy, and conditions under which the results furnished were obtained. All subordinate standards, and measuring and test equipment are supported by similar data when such information is essential for achieving the required accuracy and control. All calibration equipment is traceable to the National Bureau of Standards. Table 9 details the equipment used during the test.

All test items were received, and inspected, and no visible defects were apparent. However, on installation of the ballute retarder, several failures of the band strap were experienced. A tension brittle fracture of the strap occurred with the rupture severing the entire strap width. An investigation revealed that an improper heat treatment procedure was used. After corrections were made at the contractor's site, new straps were obtained for the follow-on tests.

A simple dead weight load was applied using the setup shown in Figure 9. Loads were applied in 10 percent increments with a 5 minute stabilization period at each load, after which strain recordings were made. On reaching 100 percent of the design limit load (DLL) for both Mach conditions (0.9 and 1.2), all loads were removed, and the structure was examined for failure or permanent deformation. The structure was then reloaded to 115 percent of DLL and allowed to stabilize for 15 minutes. Again all loads were removed, and the structure was inspected. A permanent deformation at these test loads is considered a failure. In the last phase of the loading test 150 percent of DLL was applied and allowed to stabilize for 15 minutes. The structure was unloaded and inspected. At this point, permanent deformation is permitted, but no failure of primary structural members is acceptable.

Strain gages were spaced 90 degrees apart around the strap (Figure 10). When the strap was loaded, failure occurred at the main trunion point (Figure 11).

It was determined that the trunion fitting was not structurally adequate to withstand the applied loads. The contractor changed the material of the fitting, reduced the hardness obtained during heat treating, and gusset stiffeners(Figure 12). Changing the material and reducing the hardness increased the percent elongation, thus reducing the brittleness of the material at the point of failure. Excessive heat treatment increases the strength of the structure. but causes it to become more brittle until it resembles glass. Gusset plates that were added distributed the high bending moments over a larger area and reduced the load concentration.

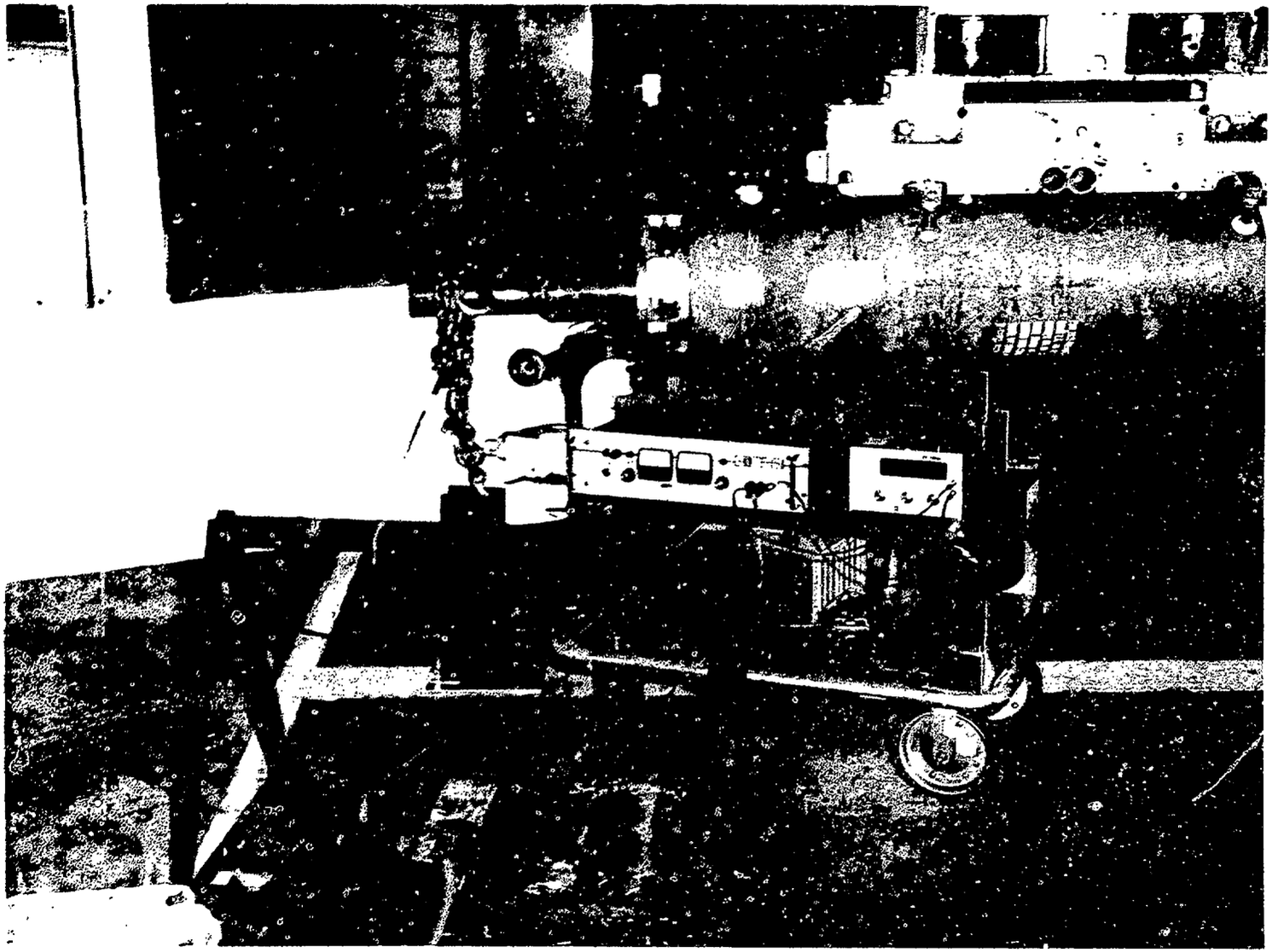

Figure 9. Static Loading

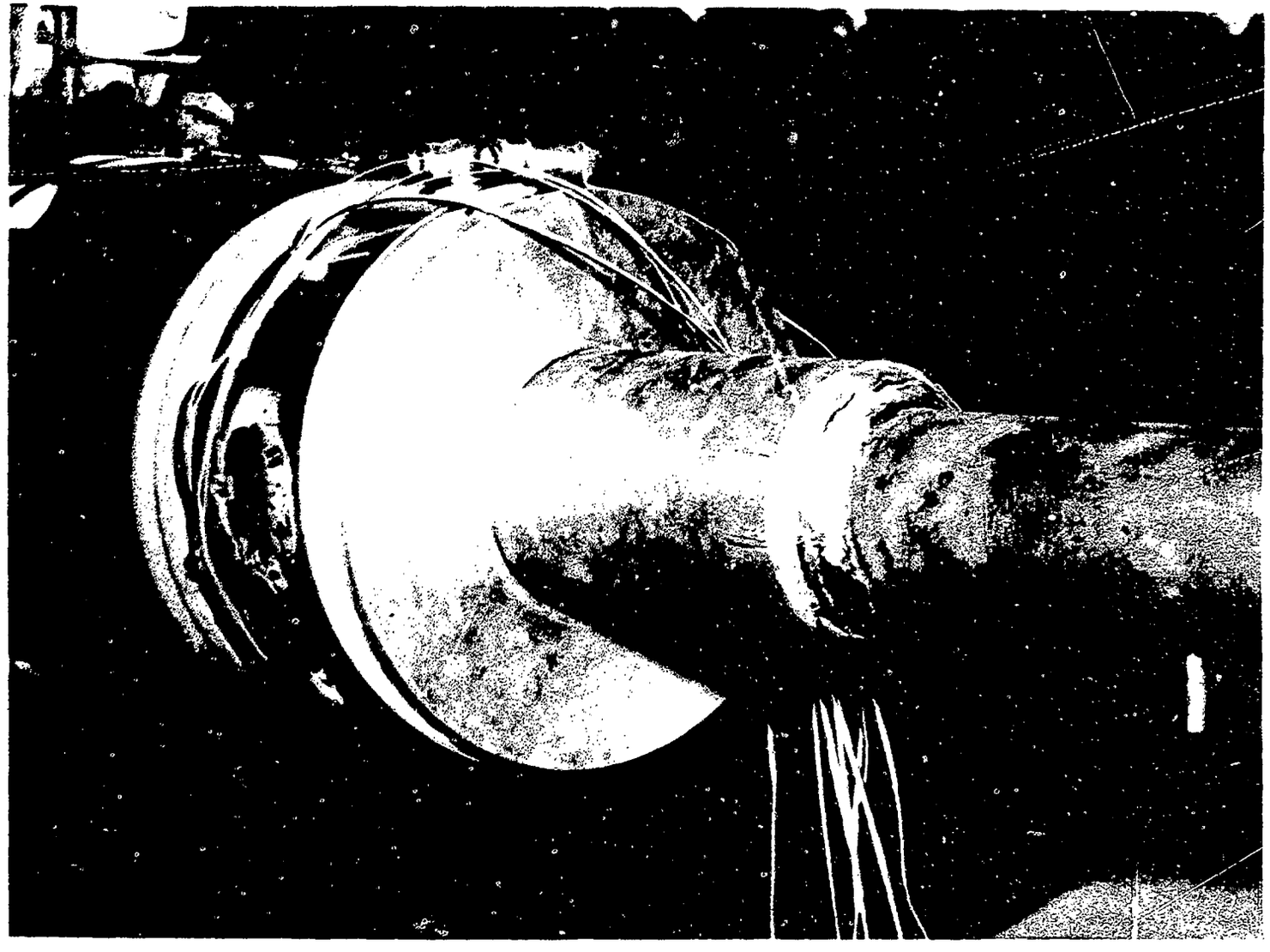

Figure 10. Installation of Strain Gages

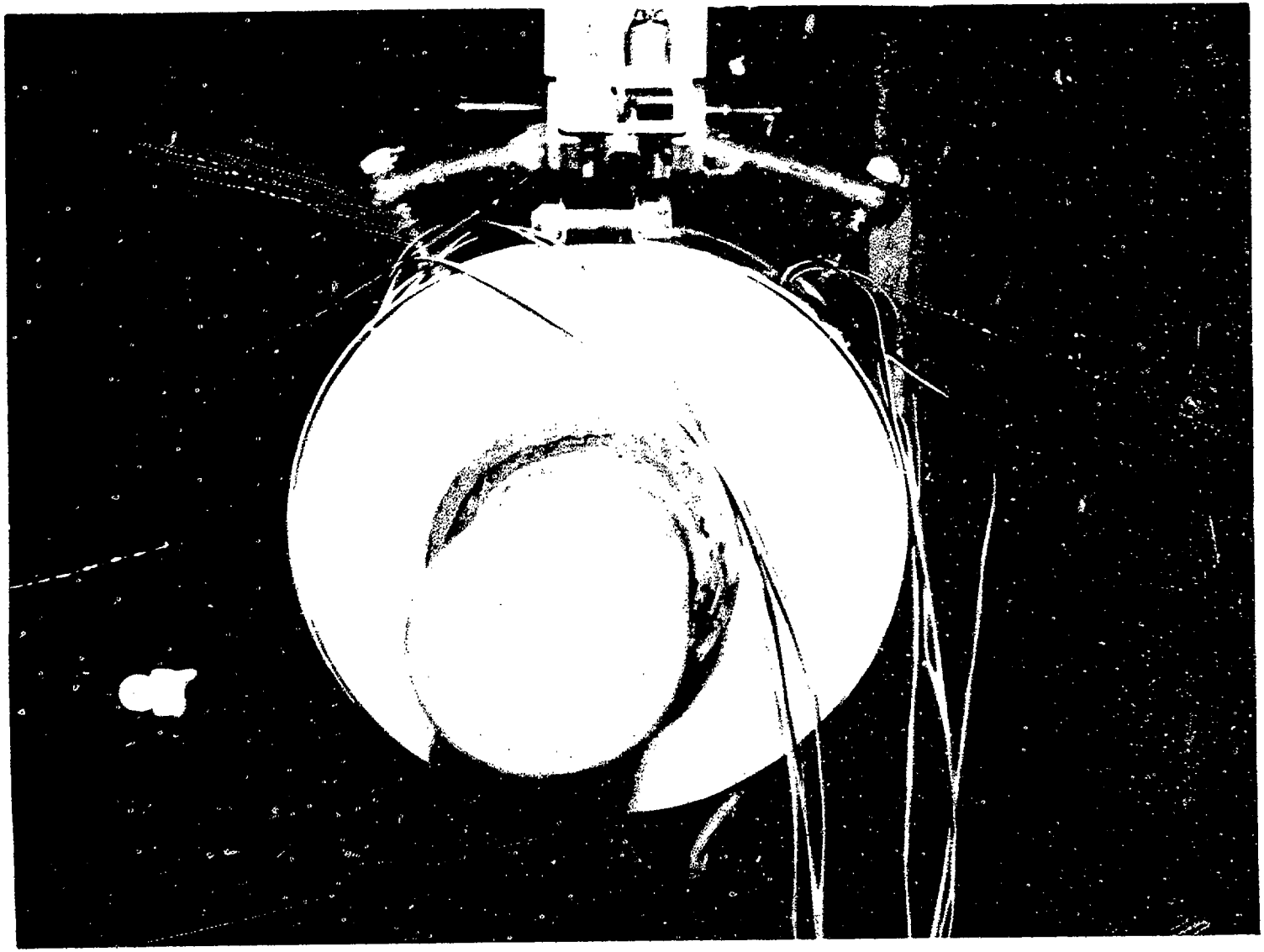

Figure 10. Continued

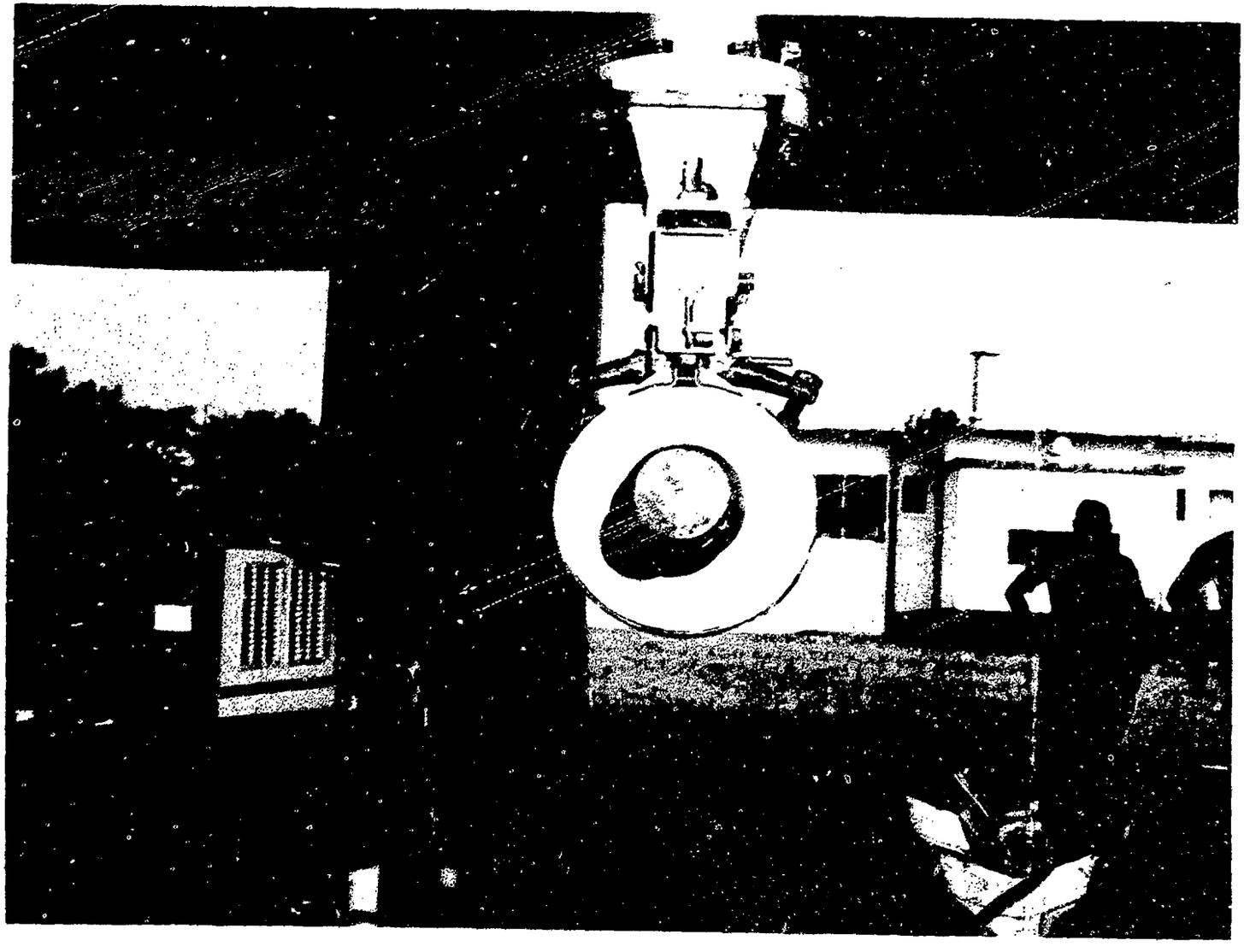

Figure 10. Concluded

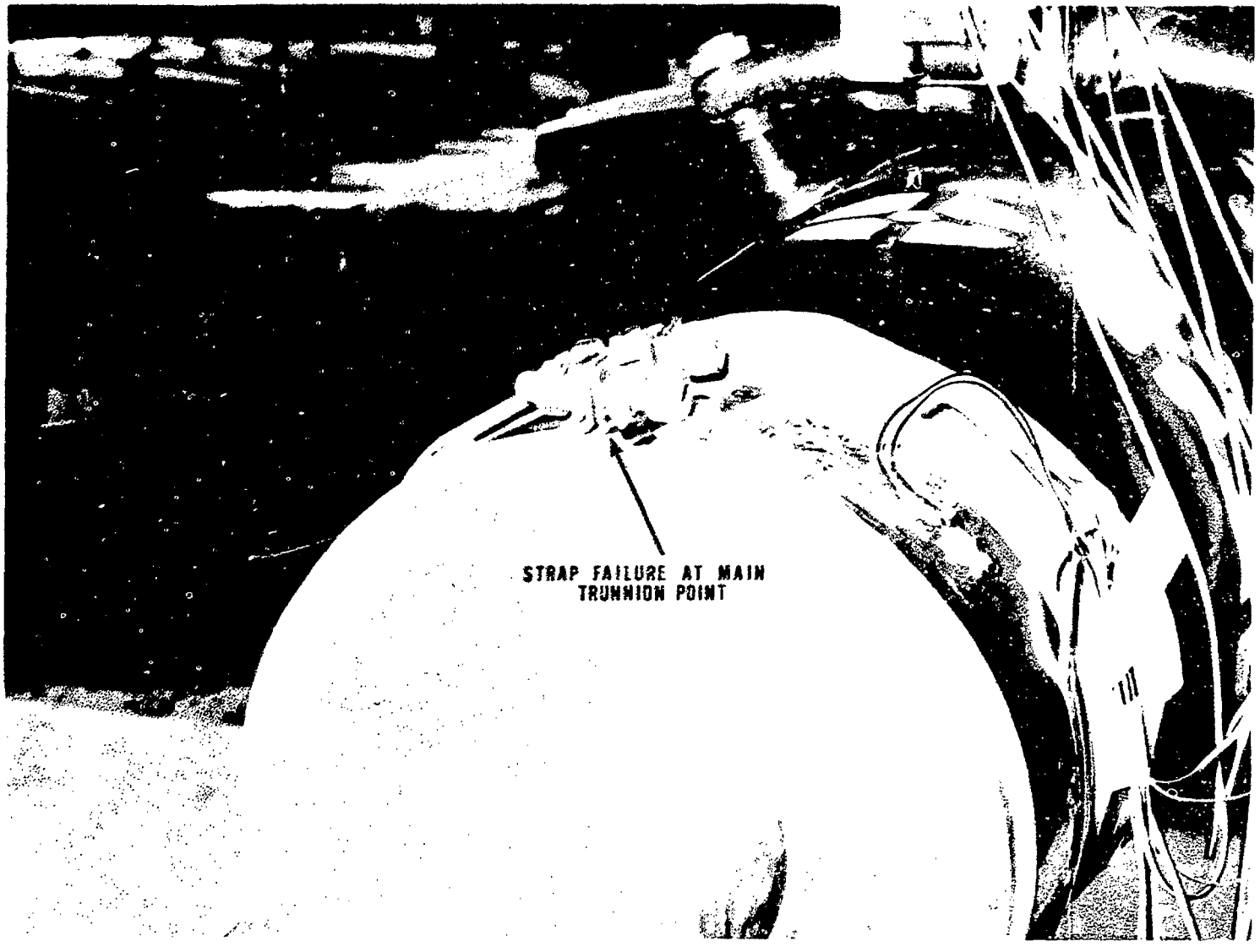

Figure 11. Failure of the Main Trunion Point

Figure 11. Continued

Figure 11. Continued

Figure 11. Concluded

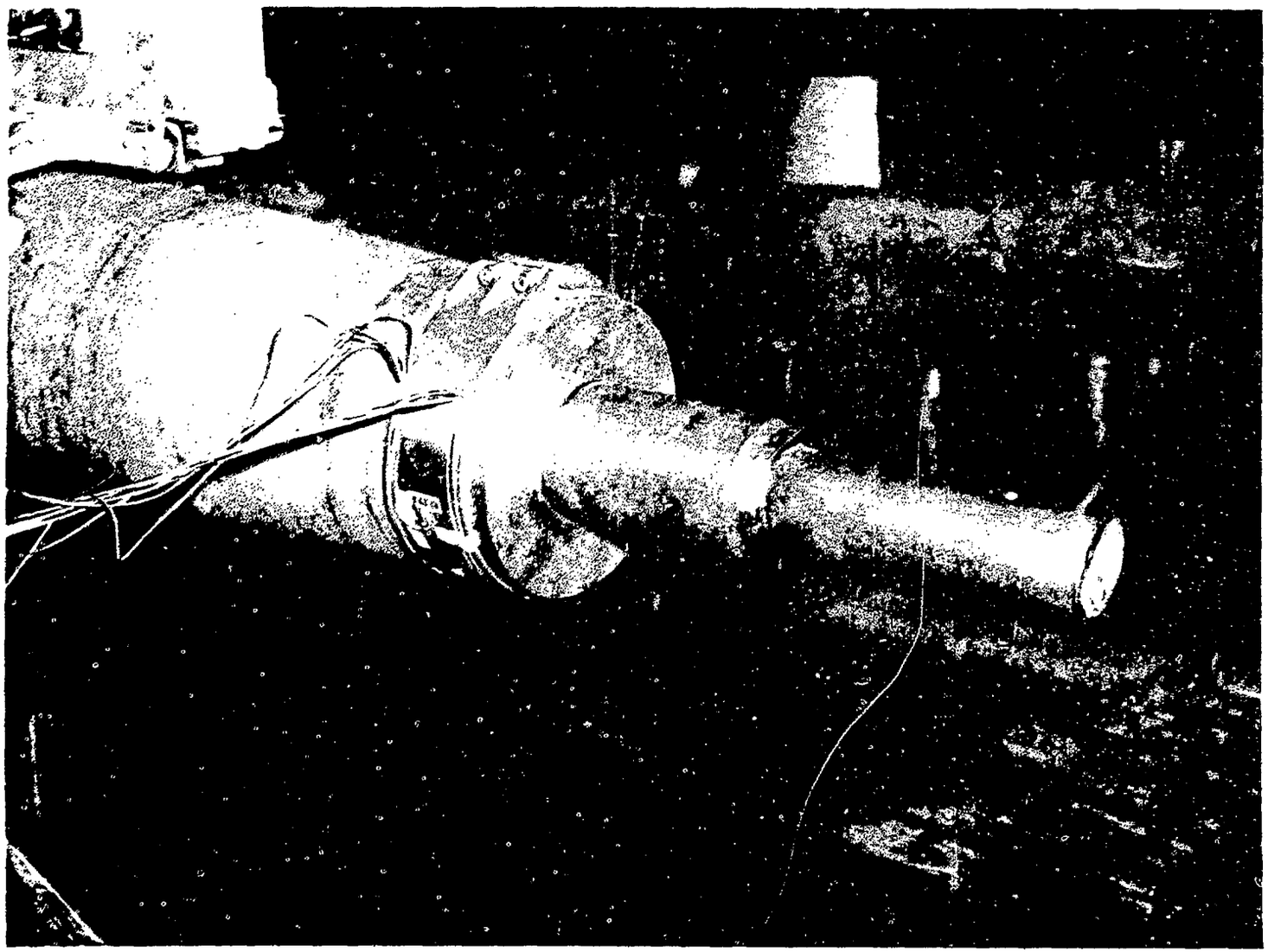

Figure 12. Final Band Clamp with Gussets

TABLE 9. TEST EQUIPMENT SUMMARY		
ITEM	MODEL	MANUFACTURER
Digital Voltmeter	X-2	Non-Linear Systems
Oscillograph	CEC 124	Bell and Howell
Power Supply	32-15	Sorensen
Galvanometer	7-318	CEC
Strain Gage	SR-4 120OC/45^{O}	BLH Electronics

When the new fin assembly was tested, it successfully completed both phases of the test for Mach 0.9 and 1.2. All loads were recorded using the strain gages, and the maximum deflection are denoted in Figures 13 and 14.

Inspection of Figure 14 will show that, after the initial loading, very little strain was experienced in the outer strap. The initial displacements resulted from seating or settling of the structure due to machining tolerances. This sudden gage sensitivity change is an indication of the rapid strain buildup that can occur in the strap when the clamp jaws are not fully in contact with the locking grooves. Failure of the strap could occur with the application of very little load (approximately 50 percent of design load) if the clamp jaws did not take the major portion of the loading. A summary of the measured strains is presented in Table 10.

Only the maximum strain displacements will be considered since very little load was actually transmitted to the strap.

$$\Delta I = \frac{SVGN}{4(R + r)}$$

Where

S = Strain μ, in/in

V = Volts applied

G = Gage factor

ΔI = Change in current, μ amps

N = Number of active gages

R = Resistance of bridge (ohms)

r = Resistance of meter (ohms)

$$S = \frac{(4)\ \mu\ (R + r)}{VGN} \quad \frac{(4)\ \mu\ (120 + 47)}{(1)\ (1.78)\ (3)}$$

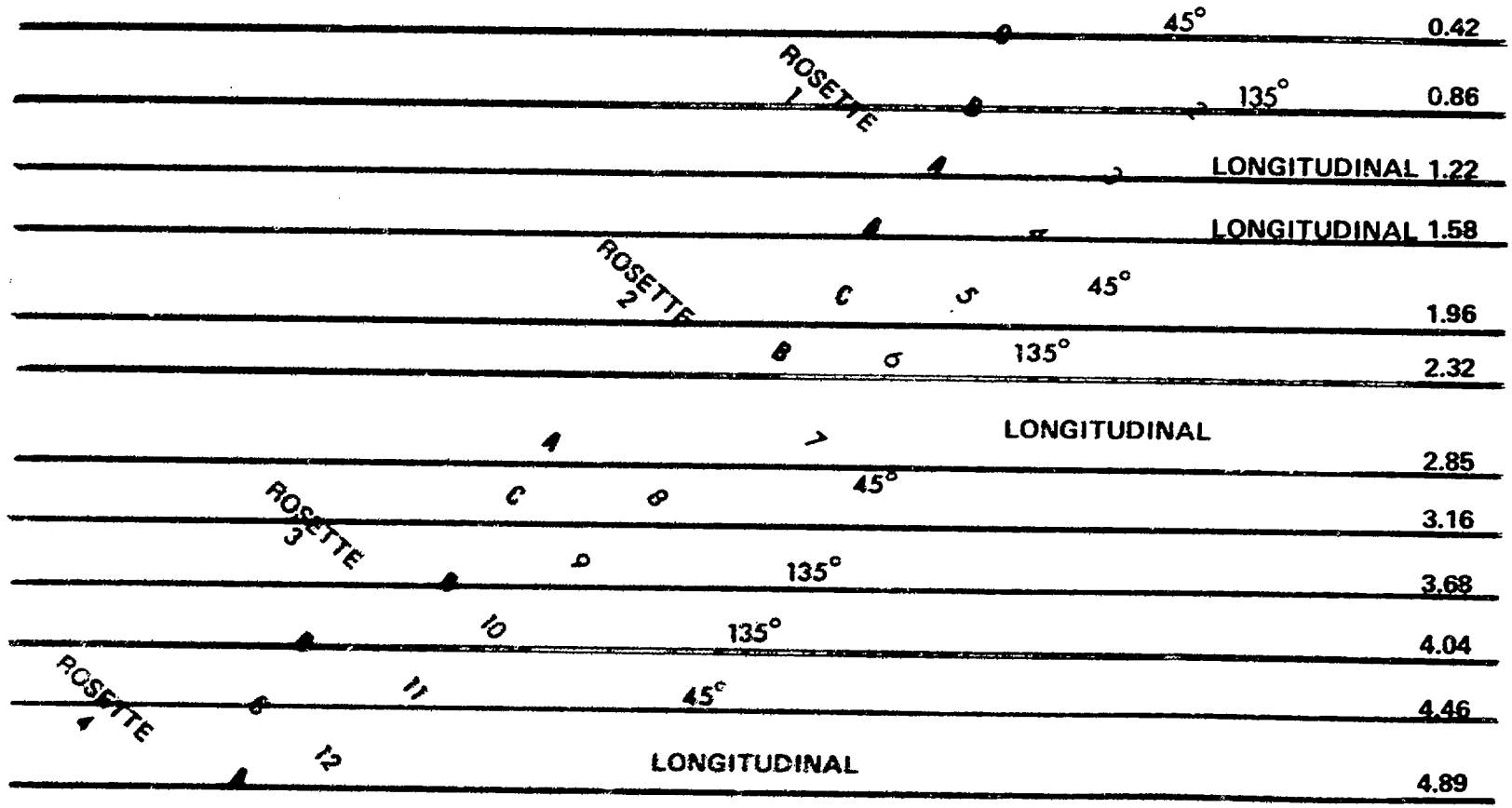

Figure 13. Calibration Check and Strain Gage Locations

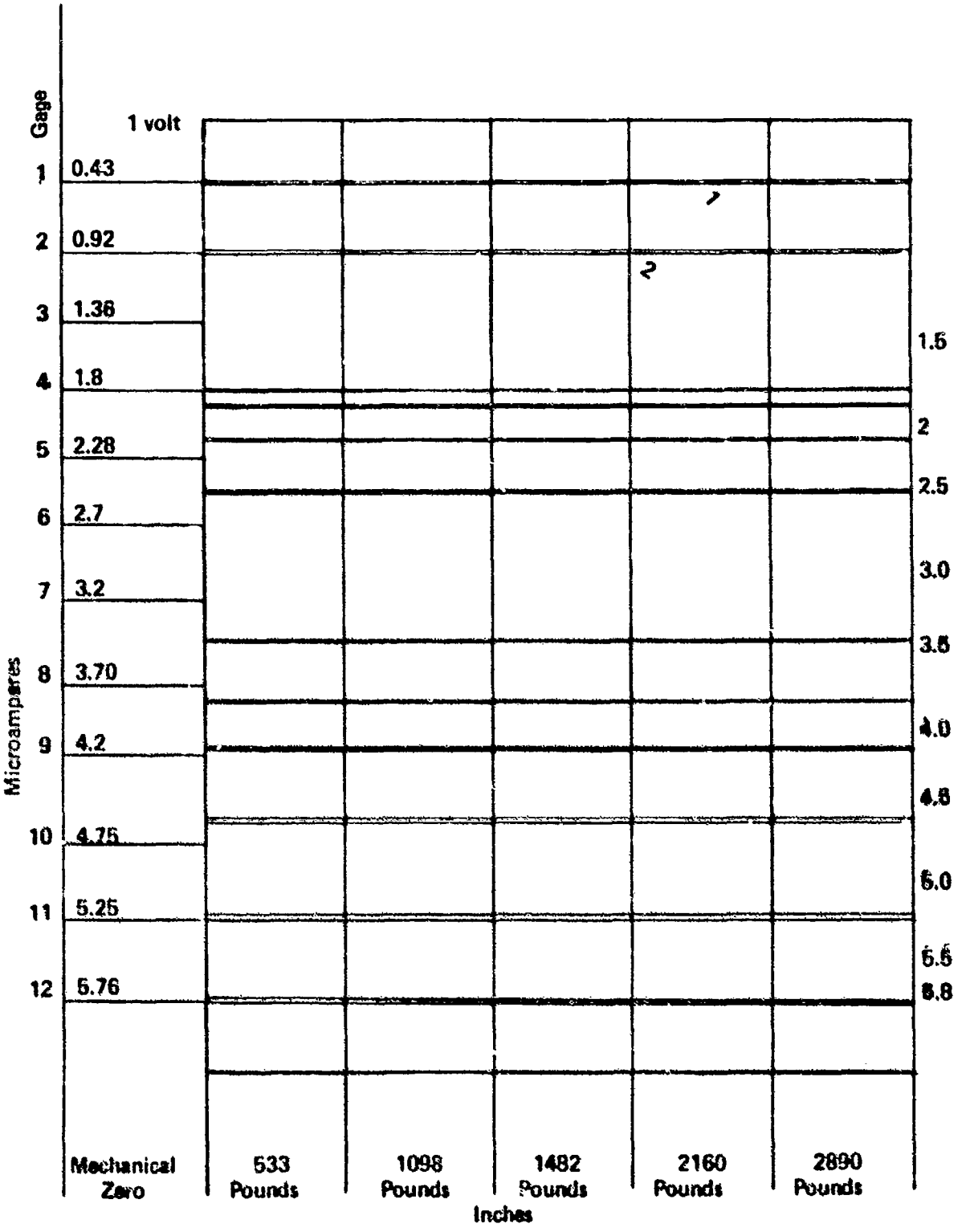

Figure 14. Strain Gage Recordings of Applied Loads

TABLE 10. MEASURED STRAIN DATA						
Gage	Element	Position	Symbol	Zero Setting	Final Setting	Δ (Amps)
A	1	45°	E_1	0.43	0.45	0.02
A	2	135°	E_3	0.92	0.94	0.02
A	3	90°	E_2	1.36	1.78	0.42
B	4	90°	E_2	1.80	1.90	0.10
B	5	45°	E_1	2.28	2.10	-0.18
B	6	135°	E_3	2.70	2.48	-0.22
C	7	90°	E_2	3.20	3.40	0.20
C	8	45°	E_1	3.70	3.83	0.13
C	9	135°	E_3	4.20	4.19	-0.01
D	10	135°	E_3	4.75	4.63	-0.12
D	11	45°	E_1	5.25	5.25	0
D	12	90°	E_2	5.76	5.82	0.06

For Gage A,

$S_3 = S_1 = 2.5\ \mu$ in/in

$S_2 = 52.5\ \mu$ in/in

The principal strains can be computed as follows (see Figure 15):

$$A = \frac{E_1 + E_3}{2}$$

$$B = \frac{1}{2}\sqrt{(E_1 - E_2)^2 + (E_2 - E_3)^2}$$

The maximum principal stress is as follows:

$$\sigma_s = \frac{E}{1 - V^2} - (B - VA)$$

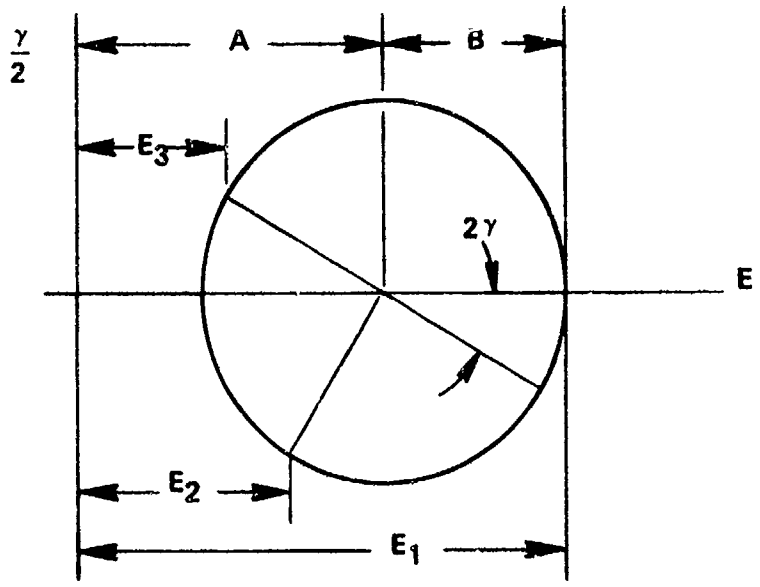

Figure 15. Mohr's Strain Circle

$$V = \frac{E}{2G} - 1$$

Where:

σ_s = Maximum principal stress lb/in^2

E = Young's modulus of elasticity

V = Poisson's ratio

G = Shear modulus of elasticity

$$\sigma_s = \frac{E}{\frac{E^2}{4G^2} \cdot \frac{E}{G}} (B + VA) = 1166 \text{ lb/in}^2$$

These low shearing stresses are a clear indication that the jaws of the clamp are functioning properly and that the basic design concept is a good one.

SECTION VI

GROUND VIBRATION TEST

The ground vibration test was the final test to be accomplished on the ballute retarder fin assembly. The type of test selected to simulate the in-flight environment was random and was based on Reference 4. The test spectrum was 20 to 2000 Hz, with a maximum power spectral density of 0.04 g^2/Hz, a 6 dB build-up from 20 to 100 Hz and a 6 dB roll-off from 1000 to 2000 Hz. Installation arrangements of the fin to the shaker (Unholtz-Dickie, 6000 pound force class) in the transverse axis are shown in Figure 16. After equalization at a low G_{rms} value, the retarder system was vibrated for 30 minutes on each axis (longitudinal and transverse). No structural failures of any kind were noted on inspection of the retarder system at the completion of testing. Control placement was at the base of the clamp. Results of the energy inputs were sampled and displayed on X-Y plots (Figures 17, 18, and 19).

Reference:

4. Environmental Test Methods, Military Standard MIL-STD-810B, 15 June 1967 (Method 514.)

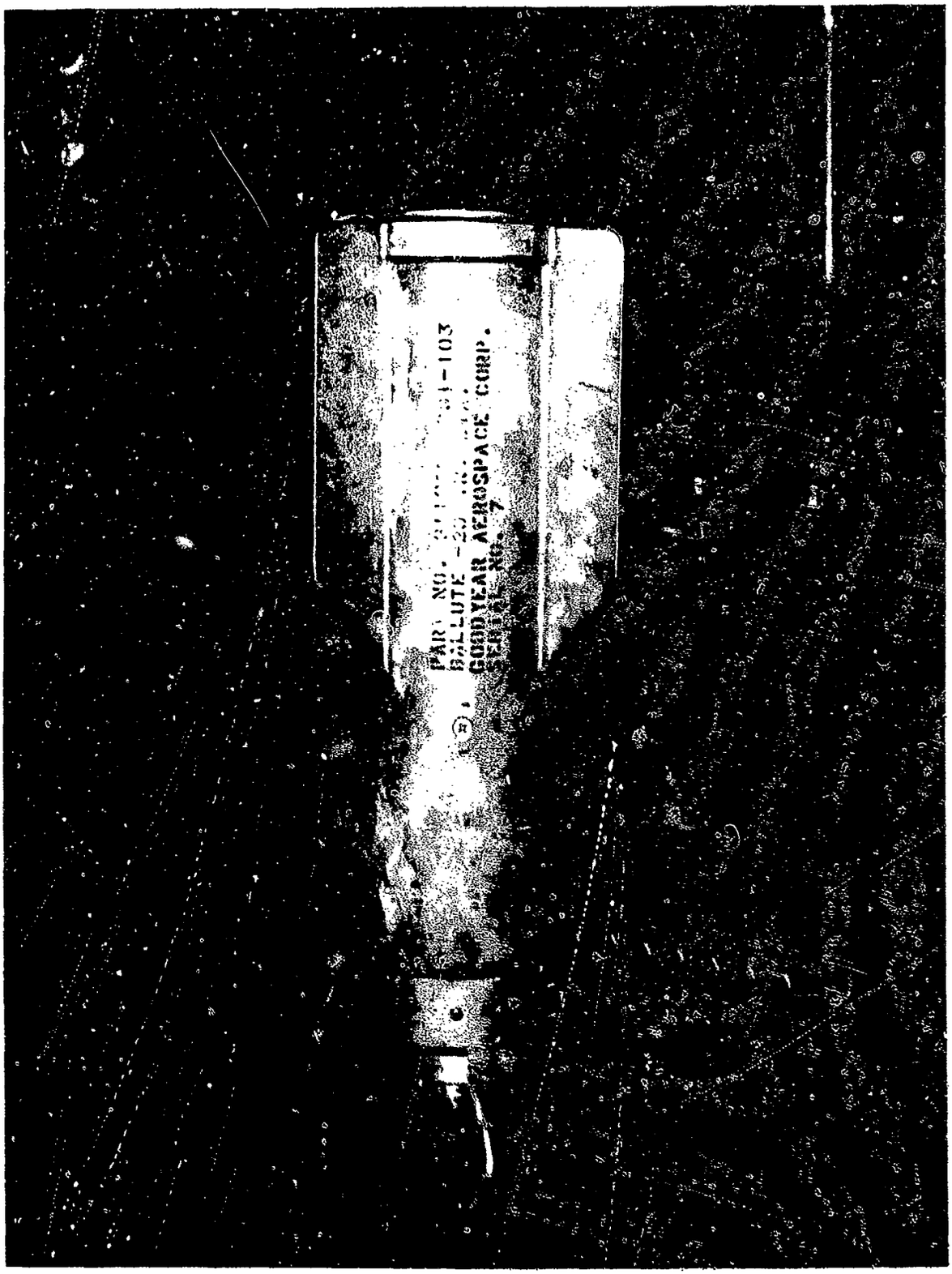

Figure 16. Vibration Test "Set-up", Transverse Axis

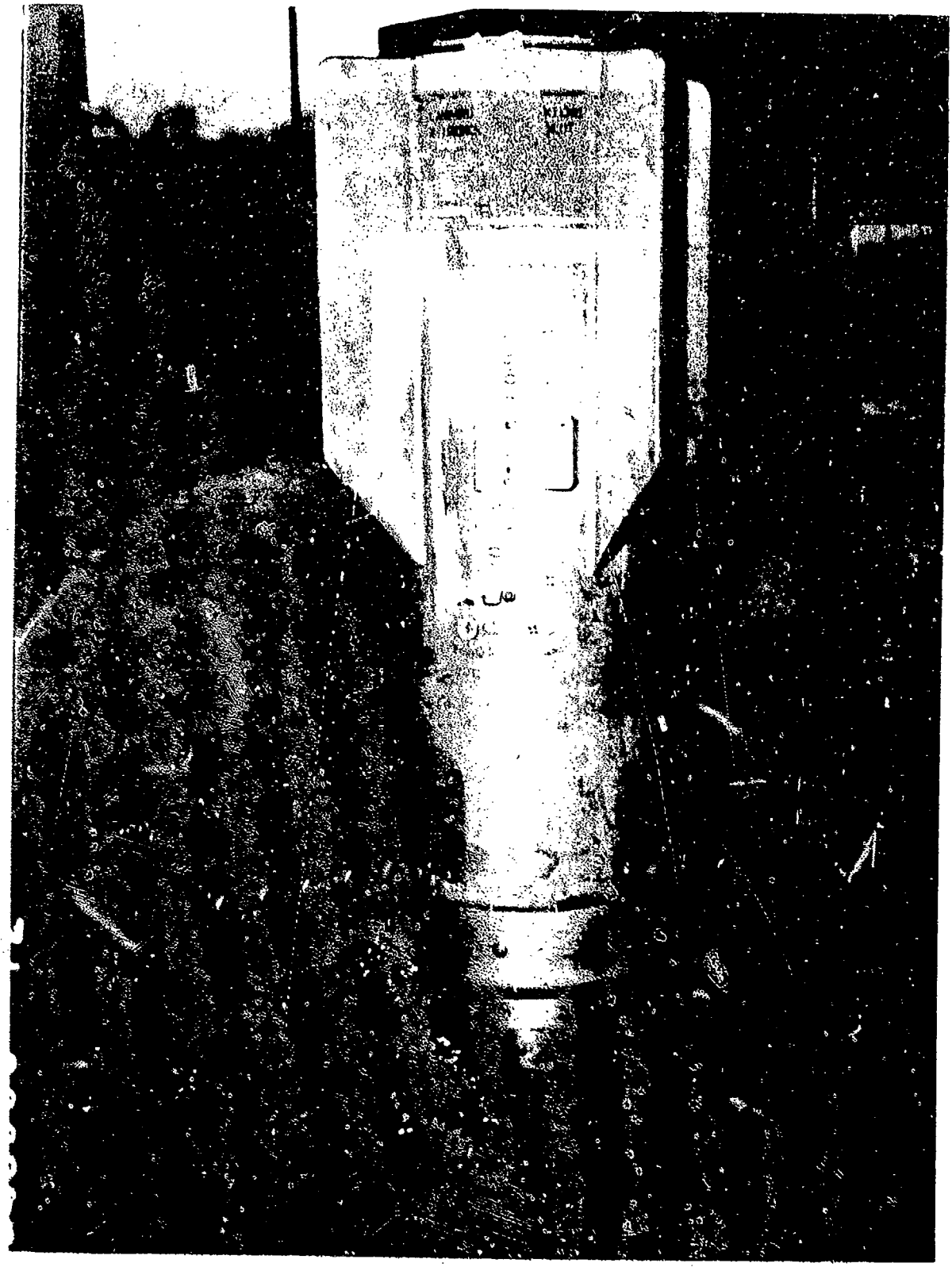

Figure 16. Concluded

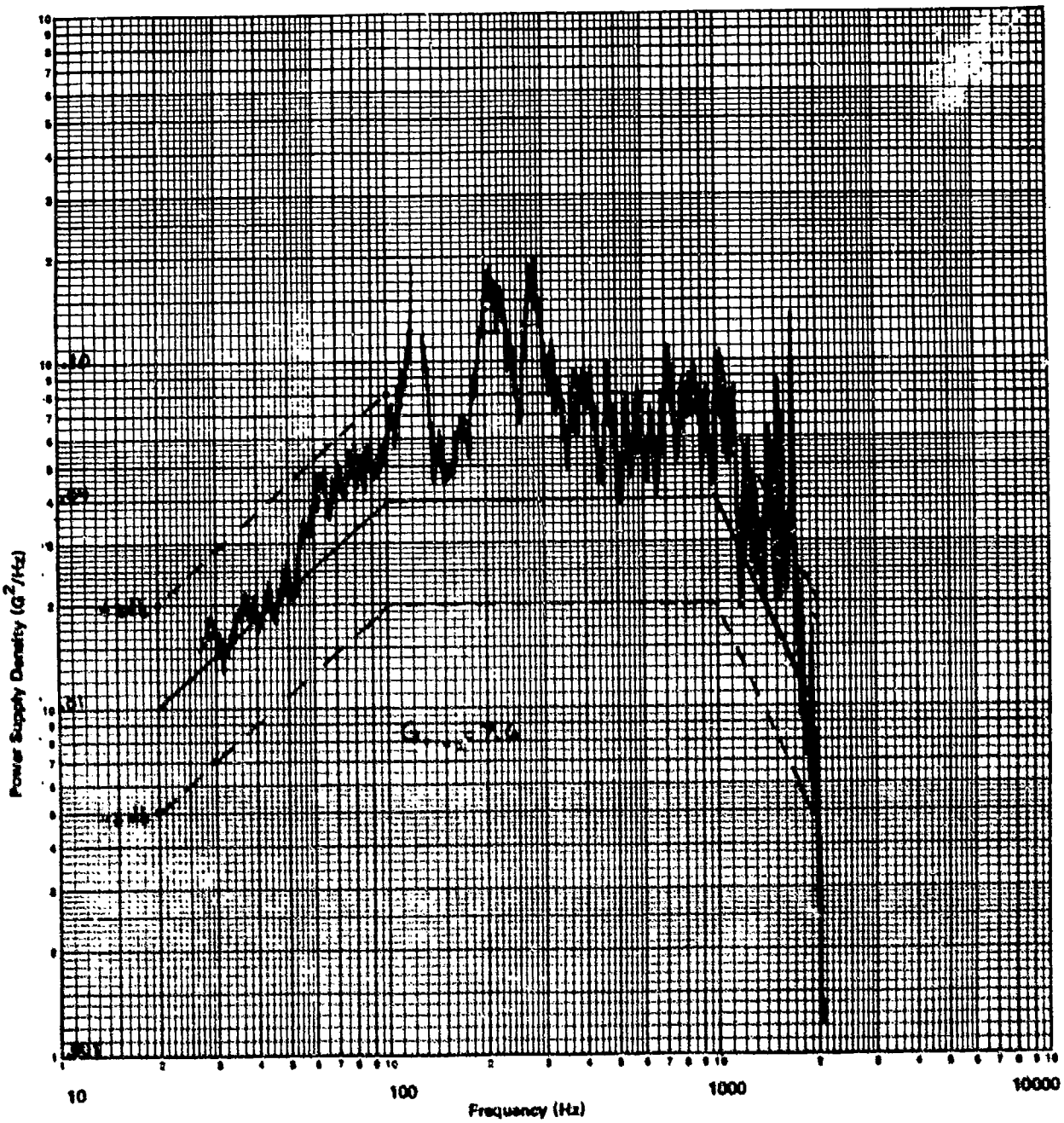

Figure 17. Energy Density for the Transverse Axis at Time = 0 Minutes

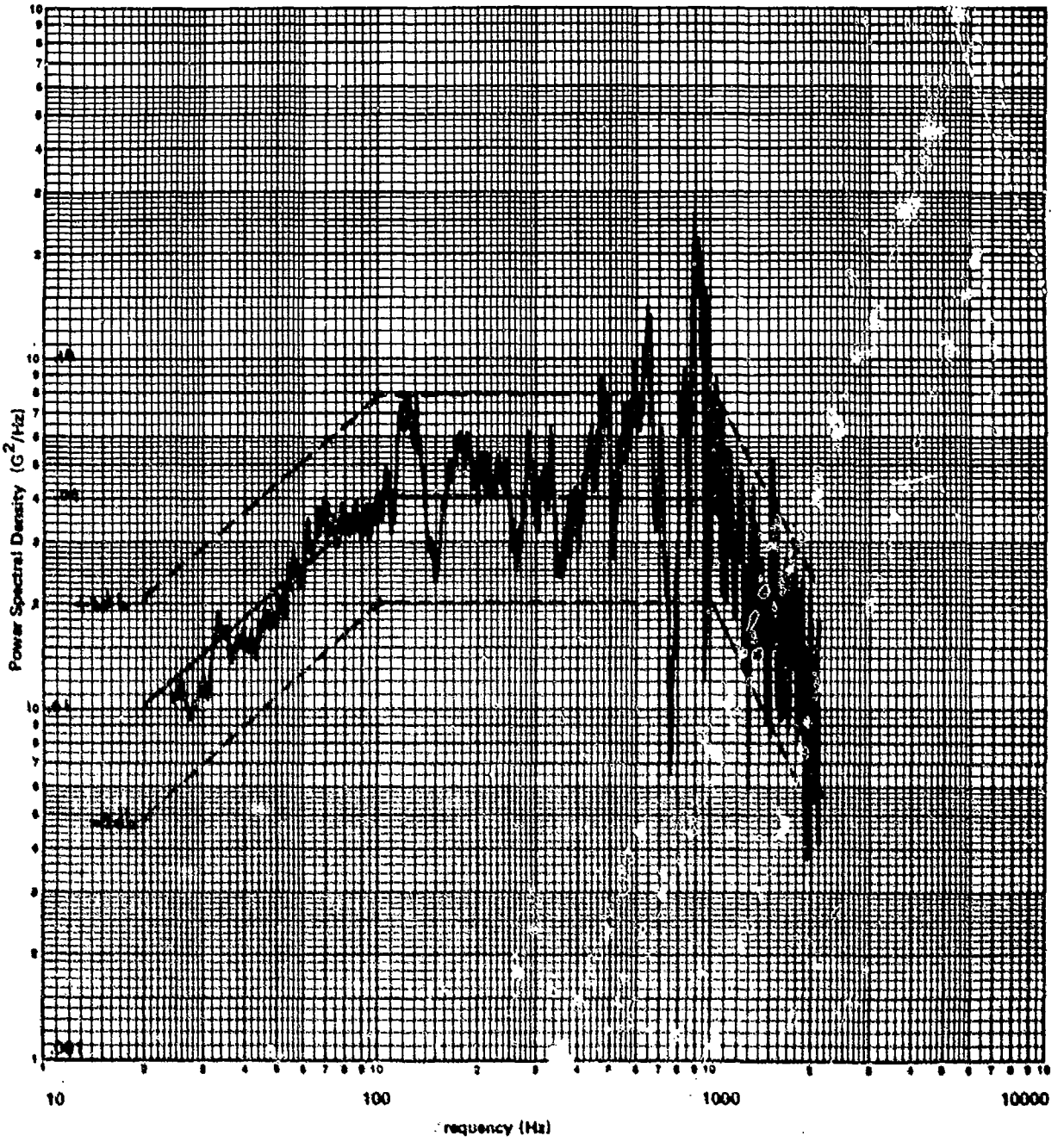

Figure 18. Energy Density for the Transverse Axis at Time = 13 Minutes

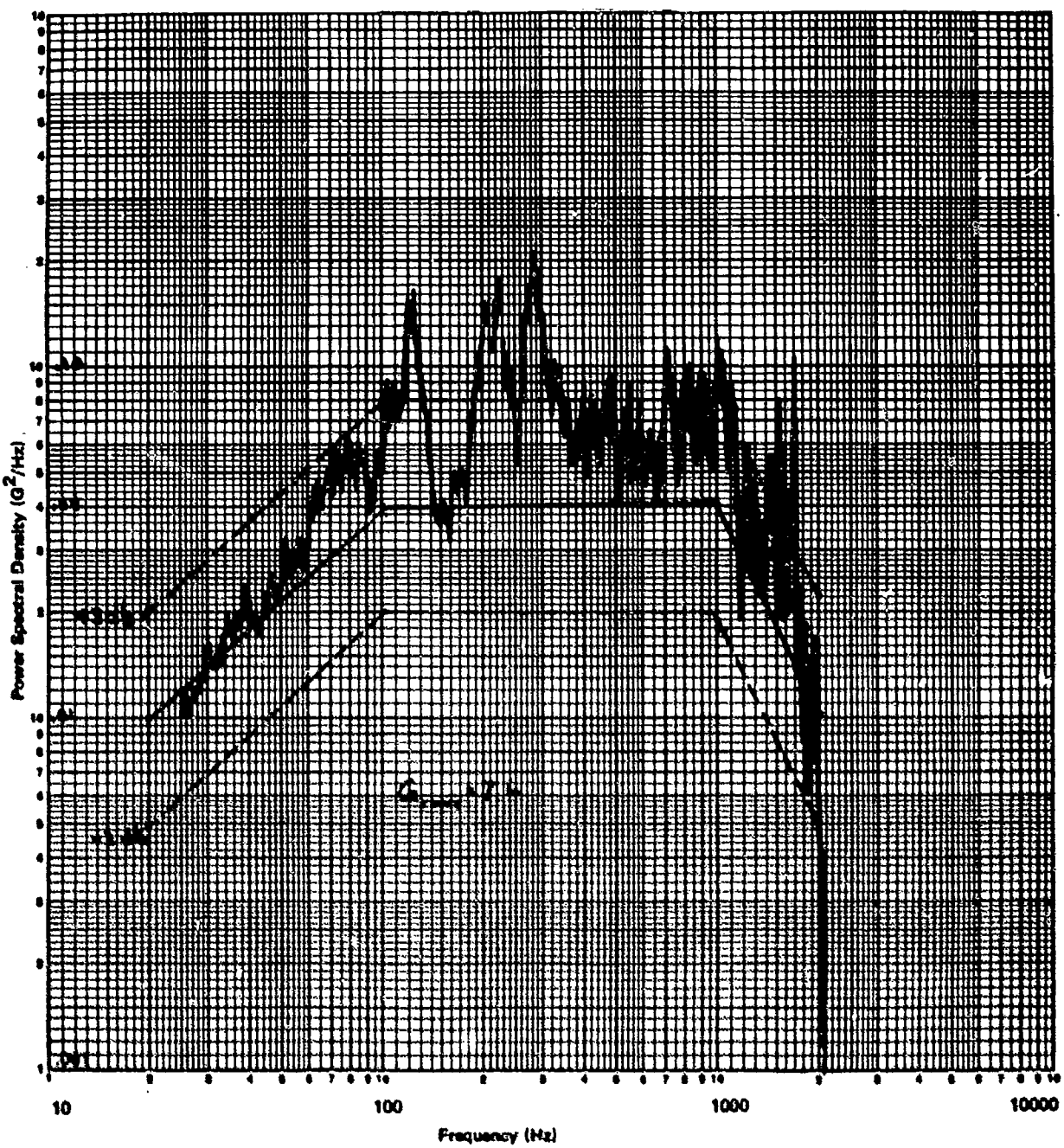

Figure 19. Energy Density for the Longitudinal Axis at Time = 12.5 Minutes

SECTION VII

SUMMARY

The analysis discussed in this report augments the contractor's completed work. Re-qualification was performed only in those areas where differences existed in the loading criteria. The failures of the originally submitted band clamp justified the additional analyses and testing.

The final design version of the band clamp successfully passed all qualification tests. At the completion of these analyses and ground tests, the ballute retarder system was successfully flight tested, including several releases for both the 29 inch and 41 inch retarder devices. A flight test summary report will be published as a separate document after completion of all flight tests.

APPENDIX A

METHOD FOR ANALYTICALLY CALCULATING THE INTERFACE STATIC LOADS

(The reverse of this page is blank)

The basic equations used in "AIRSAR" (Reference 2) are outlined in this appendix. The derivation of these equations are omitted for brevity. In addition to the symbols defined in Section III, the following are used in this appendix:

SYMBOL	DEFINITION
$\bar{R}^f_{max}$ (lb)	Maximum reaction of a forward sway-brace
$\bar{R}^f_{min}$ (lb)	Minimum reaction on a forward sway-brace
$\bar{R}^a_{max}$ (lb)	Maximum reaction on an aft sway-brace
$\bar{R}^a_{min}$ (lb)	Minimum reaction on an aft sway-brace
$\bar{V}^f_{\beta y,m}$ (lb)	Vertical component of the forward sway-brace reaction due to side load and yawing moment
$\bar{V}^a_{\beta y,m}$ (lb)	Vertical component of the aft sway-brace reaction due to side load and yawing moment
$R^{f'}_z$ (lb)	Trial forward lug reaction in the Z-direction
$R^{a'}_z$ (lb)	Trial aft lug reaction in the Z-direction

Loads at the center of gravity are based on aerodynamic and inertial considerations.

$$P_{xn} = C_d\ q\ S_{ref} + n_z W$$

$$P_{zn} = C_{n\alpha}\ \alpha_s\ q\ S_{ref} + n_z W$$

$$P_{yn} = n_y\ W - C_{y\beta}\ \beta_s\ q\ S_{ref}$$

$$M_{yn} = (q\ S_{ref})\ (C_{n\alpha}\ \alpha_s\ \ell + C_{mo}\ \ell + C_{n\alpha}\alpha_s\ X_{cp} - C_d\ Z_{cp}) + \frac{\ddot{\theta} I}{386}$$

$$M_{zn} = \frac{\ddot{\psi} I}{386} - (q\ S_{ref})\ (C_{n\beta}\ \beta_s \ell - C_{y\beta}\ \beta_s\ X_{cp} - C_d Y_{cp})$$

To obtain the loads at the center of gravity for arrested landing or catapult launch, simply remove the aerodynamic terms from the above equations (those including q) and adjust for the proper load factors and angular accelerations during these conditions.

The sway brace vertical component loads due to side load are:

$$\overline{V}^{f}_{P_y,\,M_z} = \left| \frac{[P_{yn}\,\ell_a\,\frac{(r+h+e)}{(r+h)} + M_{zn}]}{\text{Tan}\ \beta_f\,(\ell_f + \ell_a)} \right|$$

$$\overline{V}^{a}_{P_y,\,M_z} = \left| \frac{[P_{yn}\,\ell_f\,\frac{(r+h+e)}{r+h} - M_{zn}]}{\text{Tan}\ \beta_a\,(\ell_f + \ell_a)} \right|$$

The values of $V_{P_y,\,M_z}$ and $\overline{V}^{\beta}_{P_y,\,M_z}$ are always considered to be positive or compression. However, the algebraic sign of the quantity within the brackets indicates the brace (left or right looking forward) of each pair of sway braces which will be more heavily loaded. In calculating the sway-brace reactions for the various general loading conditions, use the following criteria.

(1) A positive sign for the quantity within the brackets indicates that $\overline{R}_{max}$ will be the left-hand brace.

(2) A negative sign for the same quantity indicates that $\overline{R}_{max}$ will be the right-hand brace.

The lug side reactions due to side loads are defined as follows:

$$R^{f}_{y} = \frac{P_y\ e\ \ell_a}{(r+h)\ (\ell_a + \ell_f)}$$

$$R^{a}_{y} = \frac{P_y\ e\ \ell_f}{(r+h)\ (\ell_a + \ell_f)}$$

The algebraic signs of R^{f}_{y} and R^{a}_{y} have the same significance as the sway brace signs, i.e., a positive sign indicates that R_y acts toward the left (looking forward), and conversely, a negative sign indicates that R_y acts toward the right.

The lateral lug reactions R^{f}_{y} and R^{a}_{y} together with the lateral components of the sway brace reactions, are in static equilibrium with the applied net side force P_{yn}. It can be demonstrated, however, that for values of e other than zero, equilibrium does not exist for roll moment about the X axis. Reference 3 apparently chooses not to satisfy this requirement probably due to the fact that the force system becomes redundant. The AIRSAR program contains this inconsistency, and the program user should be aware of it. Solutions obtained should be carefully evaluated, especially with regards to side force reactions. A proper adjustment can be made for those particular cases which will result in a sound and reasonable assessment of design loads.

1. TRIAL LUG REACTIONS

In order to determine the manner in which the suspension system will be reacted to a given set of applied forces, trial lug reactions ($R_z^{f'}$ and $R_z^{a'}$) must be calculated initially. The trial reactions are defined as follows:

$$R_z^{f'} = \frac{P_{xn}(r+c+e) - P_{xn}\,\ell_a - M_{yn} + \bar{V}^f_{Py}, M_z(\ell_a + \bar{\ell}_f) - \bar{V}^a_{Py}, M_z(\bar{\ell}_a - \ell_a)}{(\ell_a + \ell_f)}$$

$$R_z^{a'} = \frac{M_{yn} - P_{xn}(r+c+e) - P_{zn}\,\ell f + \bar{V}^f_{Py}, M_z(\ell_f + \bar{\ell}_a) - \bar{V}^f_{Py}, M_z(\ell_a - \bar{\ell}_f)}{(\ell_a + \ell_f)}$$

The algebraic signs of R_z^f and R_z^a are used to determine the applicable loading case per Table A-1.

TABLE A-1. ALGEBRAIC SIGNS OF TRIAL REACTIONS

Algebraic Signs of Trial Reactions		Loading Case Type	Reactions Provided
$R_z^{f'}$	$R_z^{a'}$		
+	+	I	Forward and aft lugs loaded
+	-	IIa	Forward lug and aft brace loaded
-	+	IIb	Aft lug and forward brace loaded
-	-	III	Forward and aft braces loaded

2. LUG AND SWAY BRACE REACTIONS

The final lug and sway brace reactions are determined by the following equations which are unique for each loading case type.

(a) Case I Solution - Both Lugs Loaded

$$R_z^f = R_z^{f'}$$

$$R_z^a = R_z^{a'}$$

$$\bar{R}^f_{max} = \frac{\bar{V}^f_{P_Y}, M_Z}{\cos \beta_f}$$

$$\bar{R}^f_{min} = 0$$

$$\bar{R}^a_{max} = \frac{\bar{V}^a_{P_Y}, M_Z}{\cos \beta_a}$$

$$\bar{R}^a_{min} = 0$$

(b) Case IIA Solution - Forward, Lug and Aft Sway Brace Loaded

$$R^f_z = \frac{P_{xn}(r + \quad + e) - P_{zn}\,\bar{\ell}_a - M_{yn} + \bar{V}^f_{P_Y}, M_z(\bar{\ell}_a + \bar{\ell}_f)}{(\ell_f + \bar{\ell}_a)}$$

$$R^a_z = 0$$

$$\bar{R}^f_{max} = \frac{\bar{V}^f_{P_Y}, M_z}{\cos \beta_f}$$

$$\bar{R}^f_{min} = 0$$

$$\bar{R}^a_{max} = \frac{P_{zn}\,\ell_f + P_{xn}(r + c + e) - M_{yn} + \bar{V}^f_{P_Y}, M_z(\bar{\ell}_f - \ell_f)}{2 \cos \beta_a (\ell_f + \bar{\ell}_a)} + \frac{\bar{V}^a_{P_Y}, M_z}{2 \cos \beta_a}$$

$$\bar{R}^a_{min} = \frac{P_{zn}\,\ell_f + P_{xn}(r + c + e) - M_{yn} + \bar{V}^f_{P_Y}, M_z(\bar{\ell}_f - \ell_f)}{2 \cos \beta_a (\ell_f + \bar{\ell}_a)} - \frac{\bar{V}^a_{P_Y}, M_z}{2 \cos \beta_a}$$

(c) Case II Solution - Aft Lug and Forward Sway Brace Loaded

$$R^f_z = 0$$

$$R_z^a = \frac{M_{yn} - P_{xn}(r+c+e) - P_{zn}\bar{\ell}_f + \bar{V}^a_{p_y} M_z (\bar{\ell}_a + \bar{\ell}_f)}{(\ell_a + \bar{\ell}_f)}$$

$$\bar{R}^f_{max} = \frac{P_{zn}\ell_a - P_{xn}(r+c+e) + M_{yn} + \bar{V}^a_{p_y} M_z (\bar{\ell}_a - \ell_a)}{2\cos\beta_f (\ell_a + \bar{\ell}_f)} - \frac{\bar{V}^f_{p_y} M_z}{2\cos\beta_f}$$

$$\bar{R}^f_{min} = \frac{P_{zn}\ell_a - P_{xn}(r+c+e) + M_{yn} + \bar{V}^a_{p_y} M_z (\bar{\ell}_a + \ell_a)}{2\cos\beta_f (\ell_a + \bar{\ell}_f)} - \frac{\bar{V}^f_{p_y} M_z}{2\cos\beta_f}$$

$$\bar{R}^a_{max} = \frac{\bar{V}^a_{p_y} M_z}{\cos\beta_a}$$

$$\bar{R}^a_{min} = 0$$

(d) Case III Solution - Neither Lug Loaded

$$R_z^f = 0$$

$$R_z^a = 0$$

$$\bar{R}^f_{max} = \frac{P_{zn}\bar{\ell}_a + M_{yn} - P_{xn}(r+c+e)}{2\cos\beta_f (\bar{\ell}_f + \bar{\ell}_a)} + \frac{\bar{V}^f_{p_y} M_z}{2\cos\beta_f}$$

$$\bar{R}^f_{min} = \frac{P_{zn}\bar{\ell}_a + M_{yn} - P_{xn}(r+c+e)}{2\cos\beta_f (\bar{\ell}_f + \bar{\ell}_a)} - \frac{\bar{V}^f_{p_y} M_z}{2\cos\beta_f}$$

$$\bar{R}^f_{min} = \frac{P_{zn}\bar{\ell}_f - M_{yn} + P_{xn}(r+c+e)}{2\cos\beta_a (\bar{\ell}_f + \bar{\ell}_a)} - \frac{\bar{V}^a_{p_y} M_z}{2\cos\beta_a}$$

$$\bar{R}^a_{min} = \frac{P_{zn}\bar{\ell}_f - M_{yn} + P_{xn}(r+c+e)}{2\cos\beta_a (\bar{\ell}_f + \bar{\ell}_a)} - \frac{\bar{V}^a_{p_y} M_z}{2\cos\beta_a}$$

(e) Lug Longitudinal Reactions

The longitudinal reaction at the lugs is assumed to be carried by the most heavily loaded lug (maximum R_z). The reaction is defined, for all cases, as

$$R_x = -P_{xn}$$

(The reverse of this page is blank)

INITIAL DISTRIBUTION

DDC	2
AUL (AUL-LSE-70-239)	1
ASD (ENYS)	1
PACAF (IGY)	1
USAF (RDQRM)	1
USAF (RDPA)	1
AFSC (SDWM)	1
USNWC (Code 753 Tech Lib)	1
NATC (Tech Lib)	1
TRADOC-ADTC/LO	1
AFATL (DL)	2
AFATL (DLOSL)	1
AFATL (DLJ)	1
AFATL (DLI)	1
AFATL (DLW)	1
AFATL (DLT)	1
AFATL (DLM)	1
AFATL (DLQ)	1
AFATL (DLG)	20
AFATL (DLGC)	1
AFATL (DLOU)	1
AFATL (DLB)	1
AFATL (DLK)	1
AFATL (DLD)	

(The reverse of this page is blank)